CHAPTER 1

Introduction and literature review

1.1 Introduction

Many modern industrial machines rely on vibration for their operation. Oscillatory motion is essential for screens, rock drills, compactors etc. Their proper operation demands high levels of vibration, usually to the detriment of their support structures and operators.

The combined forces imparted by the vibration of several vibratory screens simultaneously, may for example cause fatigue failure of the supporting structures and plant buildings, or may alternatively require much more expensive civil engineering infrastructure than is really necessary (Greenway, 1983).

Various techniques exist which can be employed to reduce this vibration. The most common method is the use of low stiffness and damping isolators. This method is limited by the permissible static deflection of the isolating springs. Other methods include the use of sub-frames and counterweights. These methods add a lot of mass and cost to the structure. Sub-frames will also increase the transient response of the system and counterweights will require more force to achieve the desired acceleration. This study will specifically show how vibration absorbers can be employed to reduce the amount of vibration transmitted to the support structure.

Vibration absorbers are devices used to attenuate the vibration of a primary system by adding a secondary spring and mass system (Rao, 1990). The absorber reduces the response at a tuned isolation frequency. At the isolation frequency the inertia of the secondary system is utilised to cancel the forces normally transmitted to the structure or the operator's hands. Such devices can therefore be used on machines that are primarily operated at a dominant frequency of excitation, like vibrating screens or rock drills.

A literature survey revealed that this subject has been investigated thoroughly. The most suitable absorber concept found was the Liquid Inertia Vibration Eliminator developed for helicopter rotor head vibration attenuation (Halwes, 1980). This concept uses hydraulic amplification of the absorber mass through a proper geometric arrangement. This feature is exploited to achieve isolation without the weight penalty of current screen isolation methods.

The second chapter will be devoted to finding the equations describing the absorber's isolation properties. An experimental absorber was built and tested. The design is documented in chapter three and the experimental results subsequently. In chapter five a comparison of the isolation and absorbing techniques available for screens is presented.

1.2 Vibrating machines

A wide variety of vibrating machines are used in industry to achieve a range of material handling functions. This study will specifically investigate vibrating screens. An introduction to vibrating screens is therefore necessary. This introduction will include the classification of vibrating machines, which will be used to narrow down the area of investigation. The screen motion can be characterised by angle, stroke length, frequency and stroke pattern. The motion is important since it will influence the feed rate and screening effectiveness. The motion requirements will be discussed in the paragraph on bulk solid movement theory. It is also necessary to define the terminology used in the screening industry. The basic elements of a screen will be listed. This will include the different configurations used for the isolation and forcing of screens. Next these elements will be constructed into a single degree-of-freedom mathematical model. This model will be used to show what the requirements for screen isolation are.

1.2.1 Classification of vibrating machines

Vibrating machines can be classified as follows (Frolov & Goncharevich, 1991):

- Vibrating mixers, separators and installations for compaction and loosening of disperse mediums.
- Vibration transport and processing machines.
- Vibrating elevators.
- Vibrating crushers.
- Vibration machines for strengthening treatment (i.e. surface hardening).

Frolov & Goncharevich define vibrating screens as "a variety of vibrating separators with perforated sieving surfaces". Screening units perform a function of scalping, de-dusting, grade sizing, washing or de-liquefying (Heyns & Van Niekerk, 1997). Grade sizing or classification can be done by size, shape, density, friction coefficient or other specific properties of the particles that constitute the medium. The medium can also be classified in more than one class by using multiple sieving surfaces.

Although this work will concentrate specifically on vibrating screens, the techniques developed will also be applicable to other vibrating machines operating at a constant excitation frequency.

1.2.2 Bulk solid movement theory

Particles are moved or conveyed over the screening surface through a series of hops. This motion is achieved by the application of either a circular, elliptical or uni-directional stroke as illustrated by figure 1.1.

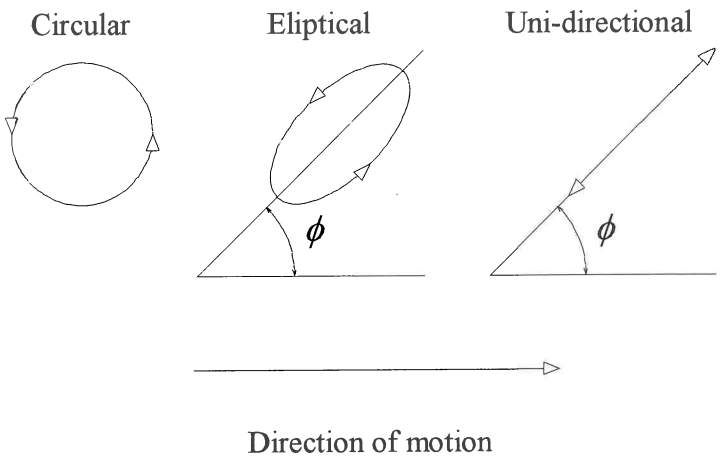

Figure 1.1 Stroke patterns (Dumbaugh, 1984)

Linear strokes are generally more efficient than either circular or elliptical strokes. A stroke angle of 30° is generally used for vibratory conveying while angles of 45° achieve better results for screening. In practice these may vary significantly according to the specific unit's function. The feed rate is a function of the stroke length and the frequency. High feed rates will diminish screening effectiveness.

Screens can be mounted on steep declines in which case a circular or elliptical stroke pattern should be used. Most often they are, however, mounted horizontally and a linear stroke pattern will be the most efficient.

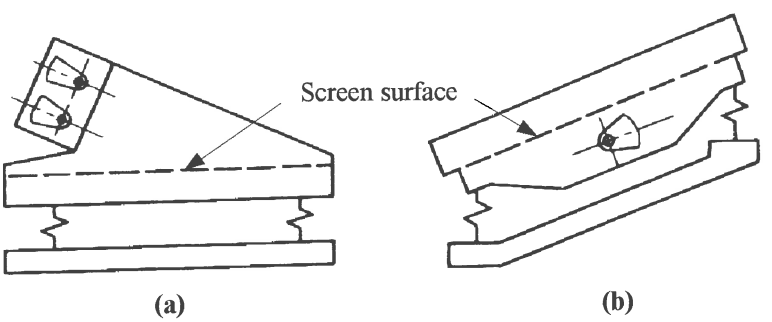

Figure 1.2 (a) Horizontal and (b) inclined screen mounting methods (Frolov & Goncharevich, 1991)

Accelerations of 3.5g are best for the conveying materials. For effective screening accelerations of between 4 and 5g are necessary (Dumbaugh, 1984). The acceleration can be achieved by varying the frequency or the stroke amplitude. Large amplitude and low frequency are used for large-sized materials and low amplitude, high frequency to size fine feeds.

1.2.3 Basic elements and configurations of vibrating screens

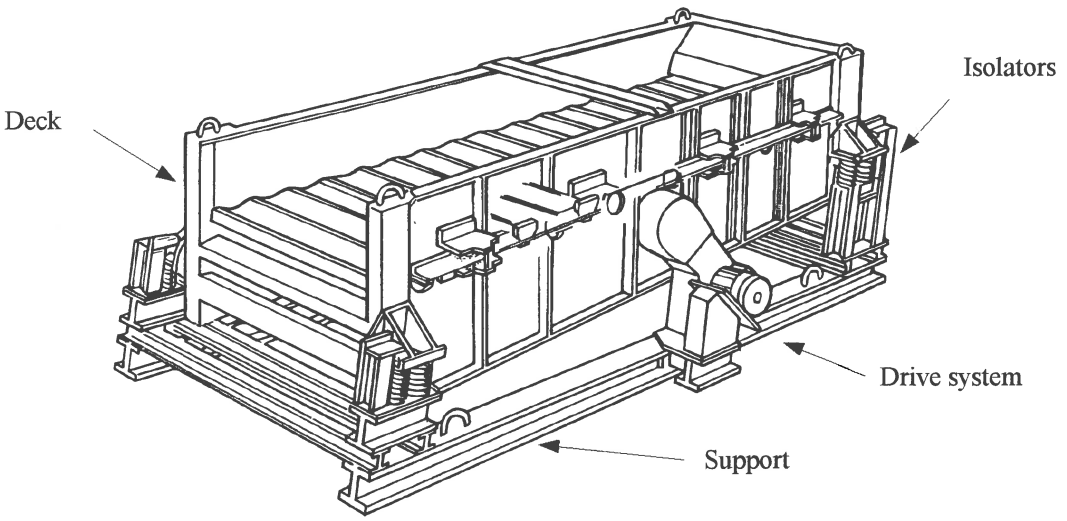

Figure 1.3 Screen elements (Frolov & Goncharevich, 1991)

The following basic elements can be identified:

- The member that contains the bulk solid is called the trough, pan, screen body or deck. More than one screening deck can be utilised to classify materials into several groups.
- The screen is exited by the vibratory drive system. Drive systems can either be linear electromagnetic shakers, rotating eccentric masses or eccentric link exciters (figure 1.4). Because of its simplicity, rotating eccentric masses are very commonly used for driving screens. To achieve linear motion, contra-rotating masses are used as shown in figure 1.2(a). Often two drives are used, one fixed with a horizontal and one with a vertical forcing direction, resulting in a 45° forcing angle.
- The screen is supported by isolation springs. Isolation springs can be either elastomeric, steel or air springs.
- The screen may be equipped with a counterweight or a sub-frame to reduce the amount of force transferred to the support

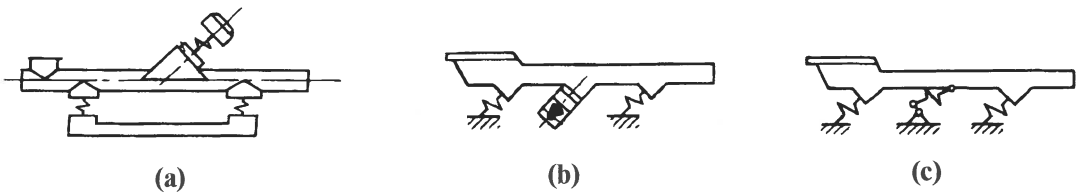

Figure 1.4 Vibratory drive systems (a) electromagnetic shaker (b) rotating eccentric masses (c) eccentric link (Frolov & Goncharevich, 1991)

1.2.4 Screen isolation assembly requirements

The objective of vibration isolation is the reduction of dynamic loads transferred to the supporting structure and the reduction of energy losses. To understand how isolator properties affect each of these it is necessary to derive a simple, single degree-of-freedom mathematical model as shown in figure 1.5.

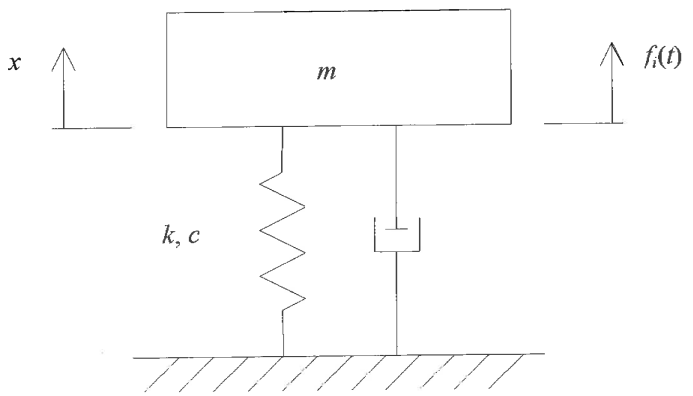

Figure 1.5 A single degree-of-freedom model of a vibrating screen

Effective isolation has the objective of low transmissibility of dynamic forces. The transmissibility is defined in terms of the applied and transmitted forces. The equation of motion is:

$$m\ddot{x} + c\dot{x} + k = f_i(t) \tag{1.1}$$

By substituting the assumed harmonic response and its derivatives, equation 1.1 can be transformed to the frequency domain (Rao, 1990):

$$\frac{X}{F_i} = \left[-\omega^2 m + i\omega c + k\right]^{-1} \tag{1.2}$$

The force transmitted to the support structure is the sum of the spring and damping forces:

$$F_o = (k + i\omega c)X \tag{1.3}$$

The transmissibility of the system is the ratio of force transmitted to the foundation (F_o) to that of the excitation force (F_i) and is shown in equation 1.4:

$$T_r = \left|\frac{F_o}{F_i}\right| = \left\{\frac{1+\left[2\zeta\frac{\omega}{\omega_n}\right]^2}{\left[1-\left(\frac{\omega}{\omega_n}\right)^2\right]^2+\left[2\zeta\frac{\omega}{\omega_n}\right]^2}\right\}^{\frac{1}{2}} \tag{1.4}$$

Equation 1.4 may be written in non-dimensional form using the well-known definitions:

$$\omega_n = \sqrt{\frac{k}{m}} \tag{1.5}$$

$$c_c = 2\sqrt{km} \tag{1.6}$$

$$\zeta = \frac{c}{c_c} \tag{1.7}$$

ω/ω_n is known as the frequency ratio.

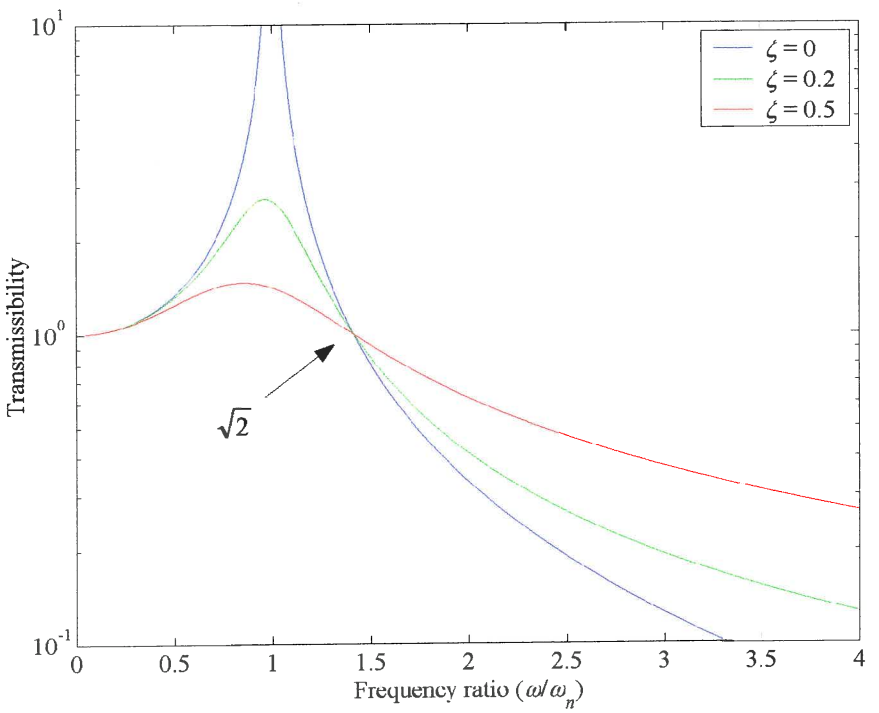

Figure 1.6 The influence of damping on the transmissibility of an isolator

For the design of a screen's isolating assembly the following requirements could be listed. (not all of these can be met simultaneously):

1. The low transfer of dynamic forces during steady state operation requires:
   - Low damping.
   - Low natural frequency, which will require low stiffness (equation 1.5).
2. The low transfer of dynamic forces during transient operation requires high damping.
3. Low static deflection requires high stiffness.
4. 4 to 5g acceleration.
5. The stresses in the springs must be low enough not to cause fatigue failure of the isolating assembly.
6. Low excitation force requires operation close to resonance.
7. Low power requirements necessitates the minimum dissipation of energy i.e. low damping.

1.3 Vibration control for vibrating screens

Vibration can be reduced in the following ways (Rao, 1990):

1. By controlling the natural frequencies of the system and avoiding resonance under external excitation.
2. By preventing excessive response of the system, even at resonance, through the introduction of damping or an energy-dissipating mechanism.
3. By reducing the transmission of excitation forces from one part of the machine to another through the use of vibration isolators.
4. By reducing the response of the system with the addition of a vibration absorber.

Agnes (1997) suggested a more basic definition and categorised all isolation attempts as either:

1. The addition of modes as will be done when adding an absorber to a system or by replacing a rigid connection with an isolator.
2. The modification of modes. This will include the addition of damping or changes in mass or stiffness.

Both these methods can either be active or passive.

A more practical classification is (Heyns & Van Niekerk, 1997):

1. Passive isolation
2. Vibration absorbers
3. Active vibration control
4. Semi-active isolation

For the purposes of this study it is suggested that vibration can either be absorbed by an inertial mass or a structure can be isolated from it. Each of these methods can be implemented in passive, semi-active or active sense. Contemporary vibration control strategies for vibrating screens use passive vibration isolators and passive vibration absorbers. The application of these methods will be discussed shortly.

1.3.1 Passive vibration isolation

Vibration isolation is achieved through the insertion of a resilient member (isolator) between the vibrating mass and the foundation as shown in figure 1.5. This method is commonly used in industry because of its relatively low cost. From figure 1.6 it is clear that operational frequencies higher than $\sqrt{2}\ \omega_n$ and low damping will result in the lowest transmissibility.

A low natural frequency is therefore desirable. This can be achieved through the use of low stiffness isolators. The natural frequency is, however, limited by the static deflection as explained by the following equation:

$$f_n = \frac{1}{2\pi}\sqrt{\frac{g}{\delta_{st}}} \tag{1.8}$$

where g is the gravitational acceleration constant.

Riddle *et al.* (1984) of the Structural Dynamics Research Corporation, in a report requested by the Anglo American Corporation, suggested that the deflection must be less than 15% of the free length for rubber isolators. For a typical screen with rubber isolators of 250 mm, δ_{st} will be 37.5 mm. Steel coil springs can be designed to have static deflections of up to 125 mm, but low axial stiffness is associated with low lateral stiffness, which can cause excessive lateral movement (Heyns & Van Niekerk, 1997). The effect of static deflection on the natural frequency is summarised in table 1.1.

Table 1.1 Natural frequency lower limits

Spring type	Static deflection [mm]	Natural frequency [Hz]
Steel coil	125	1.41
Rubber	37.5	2.57

Riddle *et al.* (1984) suggested that the natural frequency must be less than 30% of the operating frequency. A natural frequency of 25 to 33% of the operating frequency was suggested by Greenway (1983). The amount of damping is dependent on the type of isolator

used. The three types of isolators that are commonly used are steel coil springs, cylindrical solid rubber springs and Neidhart springs. Their properties are summarised in table 1.2.

Table 1.2 Comparison of isolator assemblies with a frequency ratio of 4

	Damping ratio	Isolation[1] [%]
Helical steel springs	$\eta = 0.01$	93.33
Type AB Neidhart systems[2]	$\zeta = 0.16$	89.21
Typical solid rubber spring[3]	$\eta = 0.2$	93.20

[1] $100(1 - |T_r|)$, [2] Mackie *et al.* (1997), [3] Riddle *et al.* (1984)

Pneumatic springs are known to render natural frequencies of lower than 1 Hz and may be effective, but since they are not very robust and reliable damping estimates could not be obtained they were not included in this comparison. Although steel springs provide a high amount of isolation they are prone to corrosion related fatigue failure and their low damping can be problematic during transient operation.

It would generally be advantageous for a screen to have low damping since it operates at a fixed frequency that is well above the natural frequency. A certain amount of damping is, however, required to control vibration during transients.

1.3.2 Passive vibration absorbers

The dynamic vibration absorber is a device, generating inertia, which reduces the vibration level of a protected structure (Korenev & Reznikov, 1993). Vibration absorbers can be used to achieve total isolation of a primary mass at a specific frequency by employing a secondary spring-mass system (Rao, 1990). For screens, vibration absorbers are either implemented as counterweights or sub-frames (figure 1.7). Riddle *et al.* (1984) restricted their sub-frame mass to less than 1.3 times the screen mass. Counterweights usually have weight equal to that of the screen. Both of these methods add undesirable weight to the screen assembly. Additionally the sub-frame can increase the screen motion during transients. The response should generally be less than 125% that of the response without a sub-frame.

(a) (b)

Figure 1.7 (a) A screen with a counterweight and (b) a screen with a sub-frame

The transmissibility of a system fitted with a counterweight can approach zero. A typical sub-frame design will transmit less than 10% of the screen spring force. In this study it is suggested that vibration absorbers are best suited to reduce dynamic forces and will therefore be discussed in more detail.

1.4 Vibration absorbers

1.4.1 The classic vibration absorber

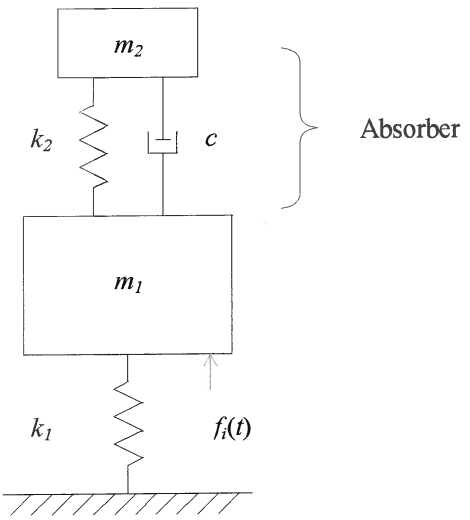

Figure 1.8 The damped dynamic vibration absorber

The classic vibration absorber was patented by Frahm in 1909. A vibration absorber consists of a primary system to which a secondary mass is added. The objective of the absorber is to minimise the motion of the primary mass. This is achieved by tuning the natural frequencies of the absorber to coincide with the excitation frequency. The result is a two degree-of-freedom system with zero response at the tuned frequency if no damping is present. This system also has two resonance frequencies, one just below and one just above the design frequency, which might reduce its effectiveness in practical applications with broad band excitation. Damping reduces the absorber's response at the resonant frequencies while also decreasing the effectiveness at the design frequency as can be seen on figure 1.9.

For most applications the added weight of the absorber will be undesirable. The mass ratio will therefore be much less than one. This implies a low stiffness and therefore a large displacement amplitude of the secondary mass. The allowable amplitude of the absorber motion will be the constraint for reducing the secondary mass. Another consideration is the effect of the mass ratio on the sensitivity to mistuning. Figure 1.10 shows that a large secondary mass will be advantageous if the primary mass is subject to changes in the

excitation frequency. In the study of vibration absorbers it is convenient to define the following ratios:

$$\mu = \frac{m_2}{m_1} \tag{1.9}$$

$$f = \frac{\omega_a}{\omega_n} \tag{1.10}$$

$$g = \frac{\omega}{\omega_n} \tag{1.11}$$

$$\omega_n = \sqrt{\frac{k_1}{m_1}} \tag{1.12}$$

$$\omega_a = \sqrt{\frac{k_2}{m_2}} \tag{1.13}$$

$$\zeta = \frac{c}{2m_2\omega_n} \tag{1.14}$$

The two important characteristic parameters for a vibration absorber are μ, the absorber's relative mass and f, the tuning ratio. The natural frequency of the primary mass is ω_n and of the absorber it is ω_a. The transmissibility is (Heyns & Van Niekerk, 1997):

$$\left|\frac{F_o}{F_i}\right| = \left\{\frac{(2\zeta gf)^2 + (g^2 - f^2)^2}{(2\zeta gf)^2\left[1 - g^2(\mu+1)\right]^2 + \left[\mu f^2 g^2 - (g^2-1)(g^2-f^2)\right]^2}\right\}^{\frac{1}{2}} \tag{1.15}$$

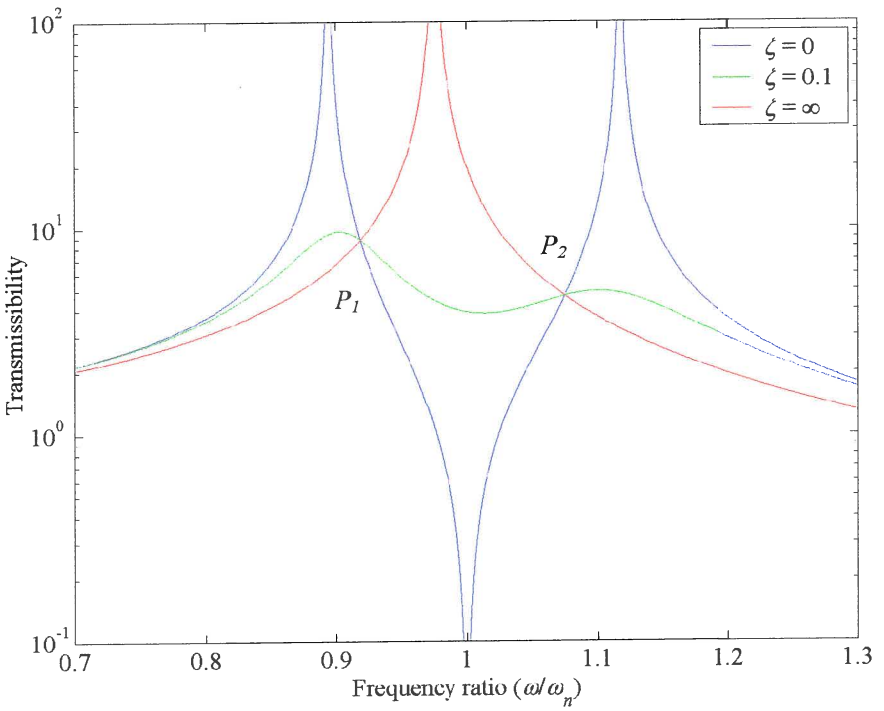

Figure 1.9 The influence of damping on the transmissibility of an absorber ($\mu = 1/20$ and $f = 1$)

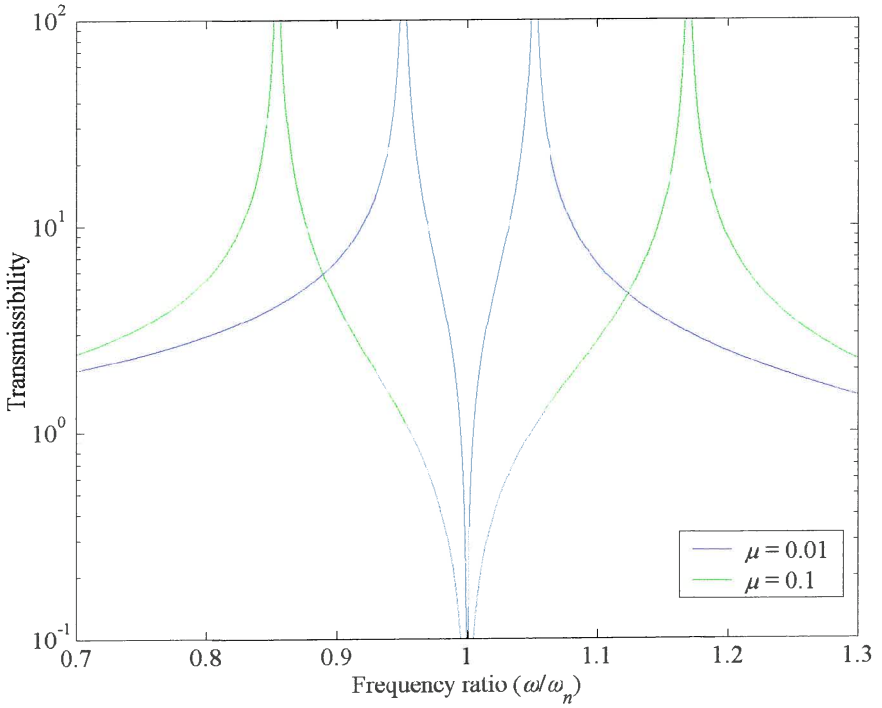

Figure 1.10 Transmissibility as a function of the mass ratio, μ ($f = 1$)

Den Hartog (1956) showed that all the curves for different damping ratios pass through the same points P_1 and P_2. Changing the ratio of natural frequencies (f) can shift the amplitude of these two points, one point going up and the other going down. The most favourable case is when the two amplitudes are equal. This was found to be (Den Hartog, 1956):

$$f = \frac{1}{1+\mu} \tag{1.16}$$

The optimum damping ratio is (Brock, 1946):

$$\zeta = \sqrt{\frac{3\mu}{8(1+\mu)}} \tag{1.17}$$

Optimal values for damped primary systems under wide band excitation are more difficult to obtain. These parameters are either given as curve fits (Tsai & Lin, 1994) or tuning diagrams (Fischer *et al.*, 1998).

Wide band excitation can also be attenuated using multiple vibration absorbers fitted to the primary structure as shown in figure 1.11. The absorbers are tuned to a range of frequencies. It is possible to increase the suppression bandwidth by increasing the number of absorbers (Igusa & Xu, 1991).

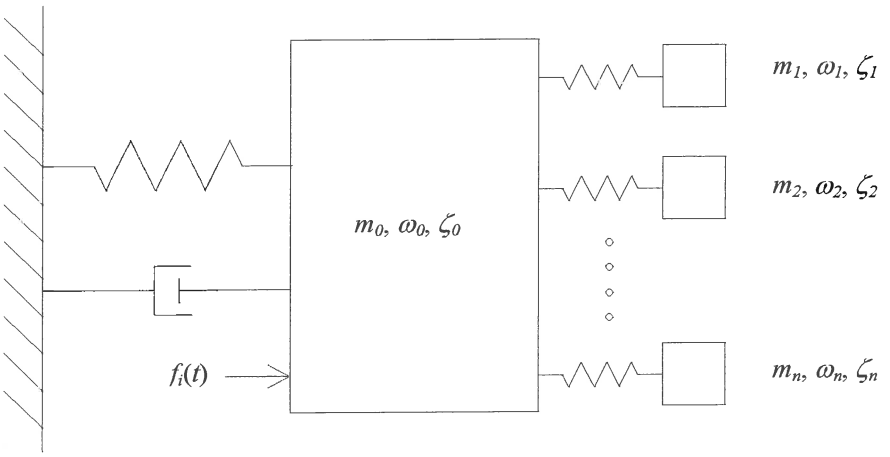

Figure 1.11 Multiple vibration absorbers in parallel

Non-linear vibration absorbers can be constructed using a non-linear stiffness element to connect the absorber to the primary mass. These absorbers have been found to increase the suppression bandwidth (Rice, 1987) and can be advantageous for sinusoidal excitation that may vary over a small frequency range. Harmonic instability can result for cases of low damping and high non-linearity.

It has also been shown that a vibration absorber can be employed to reduce the transient response of a system (Johnson, 1991). In this study the transient response was optimised so that the steepest possible decay takes place. It was found that the optimal stiffness ratio is the same as for the tuned harmonic response absorber, but that the optimal damping could be quite different.

1.4.2 Semi-active vibration absorbers

Vibration absorbers are passively tuned to match the excitation frequency. Slight variations in excitation frequency can have a significant effect on the primary system response. It is possible to decrease the sensitivity by increasing the absorber mass, but adding weight is undesirable (refer to figure 1.10). Tuning the absorber natural frequency requires that the absorber mass or stiffness be changed. O'Leary (1969) used a variable mass type absorber and reported a 1.5 Hz tuning range. Various novel tuneable stiffness designs exist. Franchek *et al.* (1995) described a coil spring with a collar that controlled the number of active coils and Margolis & Baker (1992) used the variable positioning of a fulcrum to vary the stiffness. Desanghere & Vansevenant (1991) used air pressure to adaptively tune the absorber stiffness.

It has been shown that a LR-shunted piezoceramic fixed between the primary system and the ground behaves like a mechanical vibration absorber (Agnes, 1997). Piezoelectric absorbers are tuned by changing the inductance of the RLC circuit.

1.4.3 Active vibration absorbers

It is also possible to use a positive position feedback actuator, fitted between the primary mass and the ground, to mimic a vibration absorber (Agnes, 1997). This absorber can be tuned using control system parameters. Olgac & Holm-Hansen (1993) introduced a delayed resonator where an actuator fitted between the primary and secondary masses is tuned using time delay and gain. It has been shown that the delayed resonator can reduce the primary response to zero.

1.4.4 Nodal beams and pendulums

The nodal beam concept is based on the existence of nodal points on a vibrating beam. Consider the beam response to a vertical force as shown in figure 1.12.

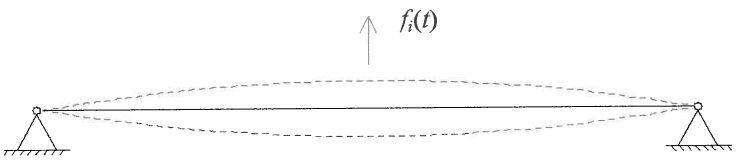

Figure 1.12. Using nodes to limit the transfer of the dynamic force

When the pinned-pinned beam is excited at its first fundamental natural frequency, two nodal points appear at the ends of the beam. Since these nodes have no motion, no force is transmitted to the ground. This property was exploited by Gaffey & Balke (1976) to produce a vibration absorber to reduce helicopter vibration. By extending the beam past the support points and adding a tuning weight to the beam's tips they were able to reduce the total weight of the absorber. The flexibility of the beam was also increased by adding a flexible joint in the middle of the beam. As soon as such a discontinuity is added the term pendulum absorber is preferred.

The Improved Rotor Isolation System (IRIS) designed by Desjardins & Hooper (1980) also used hinges and achieved 96-99% isolation during in flight testing with a weight penalty of 1.5%. The concept can be explained using figure 1.13.

At position A both the masses, the spring and inertia bar are in the neutral position. At position B the vibration of mass 1 is upward, the spring is stretched and the inertia bar is forced downward. Mass 2 remains stationary. At point D the process is reversed.

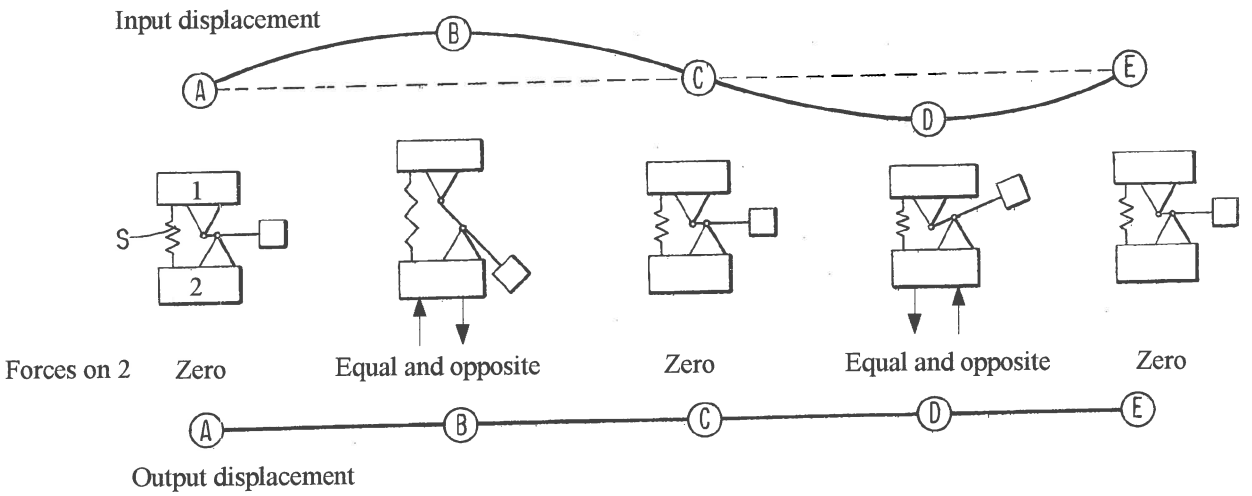

Figure 1.13 Explanation of force cancellation (Desjardins & Hooper, 1976)

It is important to note that isolation only takes place at a specific frequency. This isolation frequency can be found by analysing the equation of motion for the absorber system. A complete derivation is shown in Appendices A to C. In appendix A, a single degree of freedom system is analysed. Appendix B shows an absorber configuration added underneath a screen. Appendix C takes the effects of a flexible support into account. It is important to note which parameters influence the isolation frequency. The parameters are defined in figure 1.14 and are the two geometrical quantities, r and R, the stiffness k_1, the mass m_B and the moment of inertia of the mass m_B about its centre of gravity.

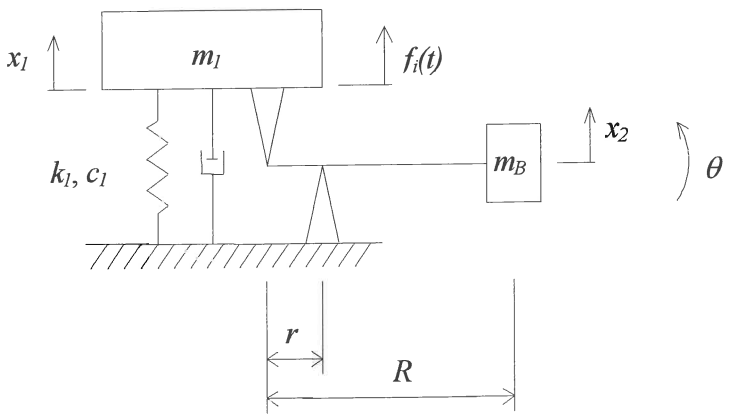

Figure 1.14 Parameters for the mechanical absorber

The complex force transmissibility is (equation A.20):

$$\frac{F_o}{F_i} = \frac{k_1 + i\omega c_1 + \omega^2\left[m_B\left(1-\frac{R}{r}\right)\frac{R}{r} - \frac{I_G}{r^2}\right]}{k_1 + i\omega c_1 - \omega^2\left[m_1 + m_B\left(1-\frac{R}{r}\right)^2 + \frac{I_G}{r^2}\right]} \tag{1.18}$$

The undamped isolation frequency is found by equating the numerator of equation 1.18 to zero:

$$\omega_a = \sqrt{\frac{k_1}{m_B\left(\frac{R}{r}-1\right)\frac{R}{r} + \frac{I_G}{r^2}}} \tag{1.19}$$

The undamped isolation frequency is independent of the system mass (m_1). This is a huge advantage for screens where the system mass may vary according to the load. Additionally the isolation frequency is a function of five parameters where the classic vibration absorber had only two tuning parameters. This gives the designer more flexibility. A comparison of non-dimensional transmissibility with and without an absorber is shown in figure 1.15. at the isolation frequency the system with an absorber's transmissibility is 33% less than for a system without an absorber. An additional advantage is the proximity to the natural frequency, which means that the spring stiffness can be increased improving the screen's stability. The force input can also be decreased while maintaining the desired acceleration.

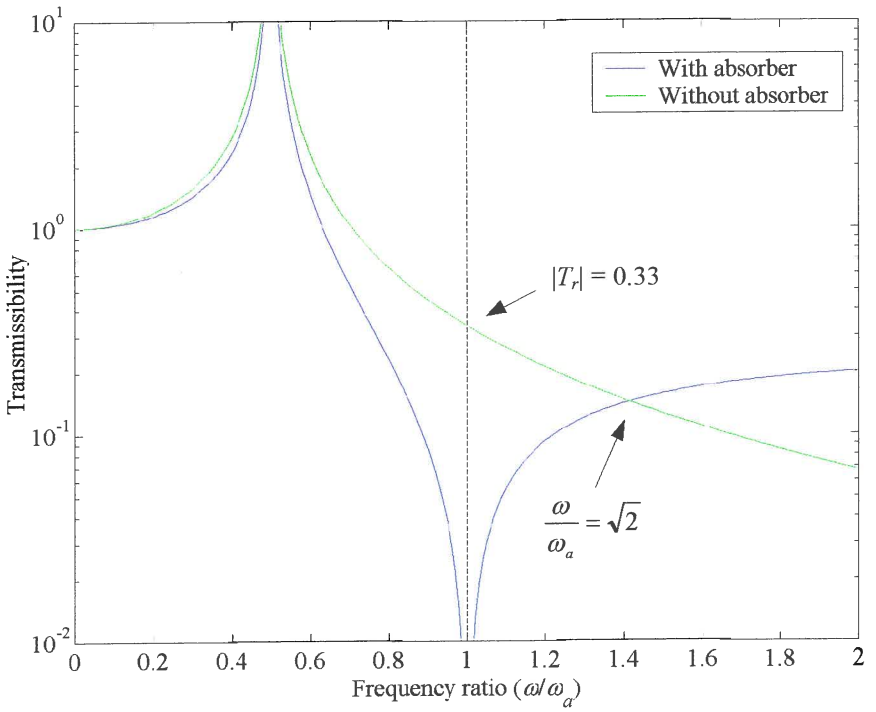

Figure 1.15 Isolator and absorber transmissibilities for systems of equal natural frequency ($\omega_a = 1$)

The practical implementation of the mathematical model is shown in figure 1.16:

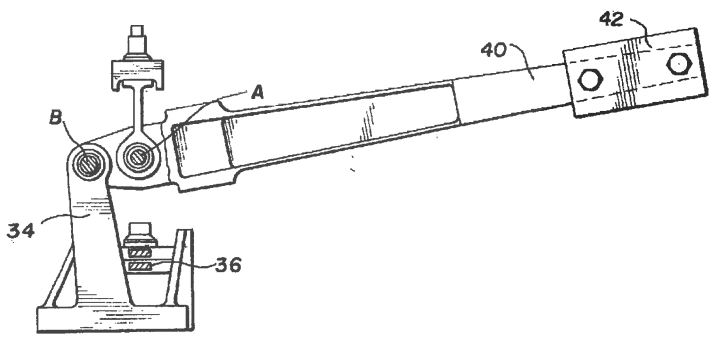

Component description	
A	Airframe pivot
B	Floor pivot
34	Anchor pad
36	Spring
40	Arm
42	Weight

Figure 1.16 IRIS for helicopter passenger floor isolator (Dejardins & Hooper, 1982)

Most of the mechanical designs have some provision for tuning after manufacture. This is usually done by moving the tip mass on the inertia bar.

This system was also improved to isolate at two frequencies by adding a spring mass system to the inertia bar as shown in figure 1.17.

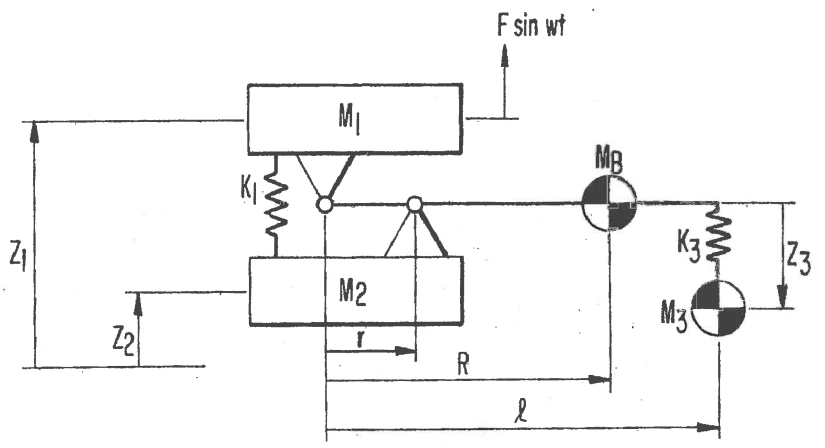

Figure 1.17 IRIS schematic for two isolation frequencies (Desjardins & Hooper, 1978)

The Dynamic Anti-resonant Vibration Isolator (DAVI) designed by Flannely (1966) operates on the same principle as the IRIS. Flannely observed that the isolation frequency could either be before or after the natural frequency of the system. Although it might seem attractive to have isolation before the natural frequency this will require a heavy absorber. Additionally, such an absorber will have a narrow bandwidth and will amplify high frequency vibrations. The DAVI was therefore designed with the isolation frequency occurring after the natural

frequency. Low isolation frequencies could be achieved with low static deflections. The importance of low damping is emphasised by figure 1.18.

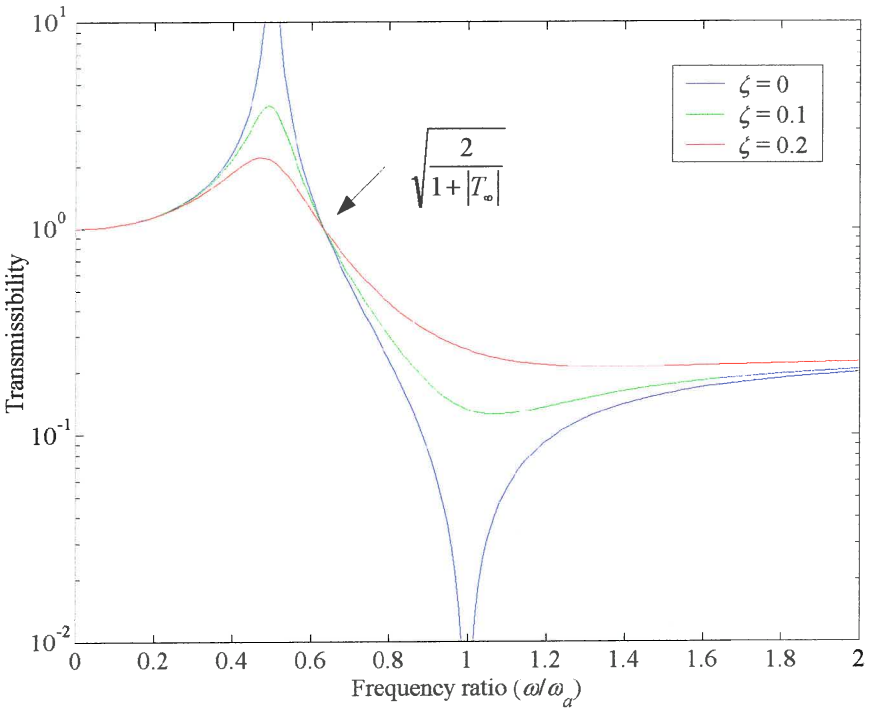

Figure 1.18 Transmissibility as a function of the damping ratio

Flannely defined the high frequency transmissibility as when the inertia terms in equation 1.18 dominates:

$$T_\infty = \frac{m_B\left(\frac{R}{r}-1\right)\frac{R}{r}+\frac{I_G}{r^2}}{m_1+m_B\left(1-\frac{R}{r}\right)^2+\frac{I_G}{r^2}} \qquad \textbf{(1.20)}$$

The high frequency transmissibility is also the ratio of the isolation to the natural frequency and will be defined such in the rest of the text. The invariant point frequency ratio ($|T_r| = 1$) is given in terms of the high frequency transmissibility:

$$\frac{\omega}{\omega_n} = \sqrt{\frac{2}{1+T_\infty}} \qquad \textbf{(1.21)}$$

For a conventional isolator this point is simply the square root of 2. It was also proved that the DAVI system would always have a response less than that of a conventional isolator having the same static deflection. The DAVI was used to isolate at 10.8 Hz. The durability of their design was proved with extensive bench and flight-testing (Rita *et al.*, 1976).

Braun (1980) published the results of the MBB Anti-Resonance Isolation System (ARIS) program. An analysis was made of different pivot bearings and it was found that elastomeric bearings provided good isolation efficiency as well as adequate radial stiffness. Braun expanded the mathematical model to include the radial and torsional stiffness and damping of the two pivots. The springs used for this design were constructed of glass fibre.

1.4.5 Hydraulic mass amplification

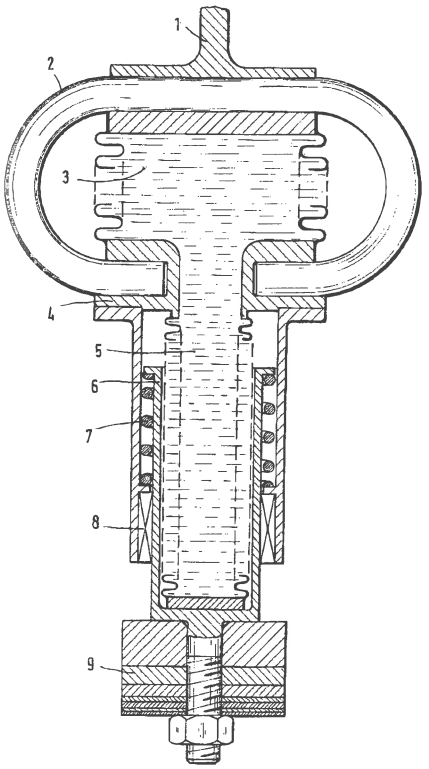

Description of elements	
1	Input force attachment
2	Glass fibre spring
3	Primary fluid chamber
4	Support
5	Secondary fluid chamber
6	Bushing
7	Spring
8	Bearing
9	Inertia mass

Figure 1.19 MBB vibration absorber (Braun, 1988)

The vibration absorber shown in figure 1.19 is essentially the same as the mechanical absorber described previously. The vibration absorber is a parallel connection of a spring and a mass with a hydraulic transmission. The absorber consists of two metal bellows and an additional glass fibre spring. The bellows form a self-containing unit and is filled with a low viscosity fluid. To minimise the flow losses it is necessary to avoid any sharp edges in the bellows system. The absorber mass is fitted to the secondary bellows and is supported by a linear bearing. The additional spring pressurises the fluid in the bellows system.

The inertia of the tuning mass causes a pressure change in the fluid chamber that acts on the vibrating mass connected to the top of the absorber and is therefore termed the force

generator. At the isolation frequency this force cancels the force imparted by the spring on the structure. The primary bellows is thick-walled in order to act as a spring. The secondary bellow is thin walled (0.25 mm) to allow large axial displacements. The isolation achieved by this design was better than 99%.

The mathematical model used was:

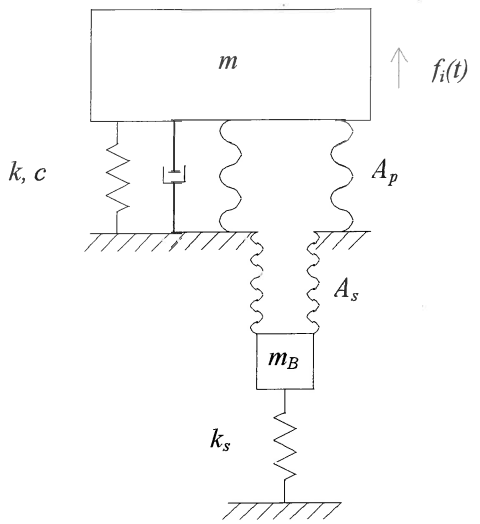

Figure 1.20 Mathematical model of the hydraulic absorber with A_p the area of the primary fluid chamber and A_s the area of the secondary fluid chamber

The undamped isolation frequency is:

$$\omega_a = \sqrt{\frac{k + k_s\left(\frac{A_p}{A_s}\right)^2}{m_B\left(\frac{A_p}{A_s} - 1\right)\left(\frac{A_p}{A_s}\right)}} \qquad \textbf{(1.22)}$$

This tuning equation differs slightly from equation 1.19 in that there is no rotary inertia present in the system and the spring k_s is amplified by the area ratio.

The advantages of this design are:

- Total symmetric arrangement of the spring and the force generator.
- Simple wear-resistant design.
- Consists of low-cost components.
- Only translational movement of the absorber mass is permitted.
- Heavily loaded pendulum bearings are not required.
- Very low damping of the spring and force generator.
- Good linearity of the isolator springs.
- Small installation space.

- Low weight.
- The force generator also allows displacement out of the isolator operating direction.
- It would be possible to add an additional spring and mass assembly for two-frequency isolation.

1.4.6 The Liquid Inertia Vibration Eliminator (LIVE)

The LIVE system was developed by Bell Helicopter Textron (Halwes, 1981). The main objective was to reduce helicopter vibrations, which contributed to crew fatigue and poor component reliability. A high-density, incompressible, low viscosity and high surface tension fluid is accelerated through a tuning port and is simultaneously used as a hydraulic fluid and an absorber mass (figure 1.21). Mercury and selenium bromide was suggested as suitable fluids. Due to relative motion between the inner and outer housing the absorber fluid is pumped through a tuning passage and generates amplified inertial forces on the inner and outer housing. At a certain frequency the inertia forces of the fluid match the spring force and the net effect is that only the damping force is transmitted. 95% isolation was achieved. The total weight penalty for the LIVE system was less than 0.75% of the helicopter gross weight. The overall size of the unit is inversely proportional to the square of the fluid density.

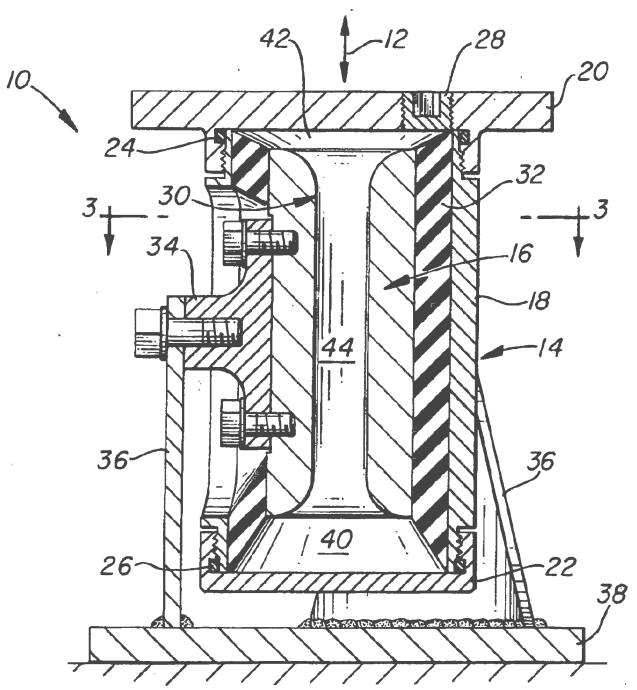

Component description	
10	Vibration isolator
12	Force direction
14	Outer housing
16	Inner housing
18	Central section
20	End section
30	Tuning cylinder
32	Elastomeric spring
38	Plate
40	Chamber
42	Chamber
44	Passage

Figure 1.21 LIVE system internal design (Halwes, 1980)

The undamped isolation frequency is:

$$\omega_a = \sqrt{\frac{k}{m_B\left(\frac{A_b}{A_a}-1\right)\left(\frac{A_b}{A_a}\right)}} \tag{1.23}$$

The advantages of this concept are:

- Reduced complexity
- Bearingless construction
- Motion safety stops inherent to the design
- Small installation envelope needed
- Linear response at high g's
- Low weight and cost
- Very low maintenance requirements

Several attempts have been made to design a semi-actively tuneable LIVE unit. Since the isolation frequency is also a function of geometric variables, there is considerably more scope for tuning than for a classic vibration absorber. Figure 1.22(a) shows an absorber with adjustable tuning port length. It is also possible to change the tuning port area by deforming a flexible member as shown in figure 1.22(b). In the same patent it is also suggested that the system damping can be decreased by adding velocity to the fluid in the tuning port. This was done using an appropriate magnetic field arrangement.

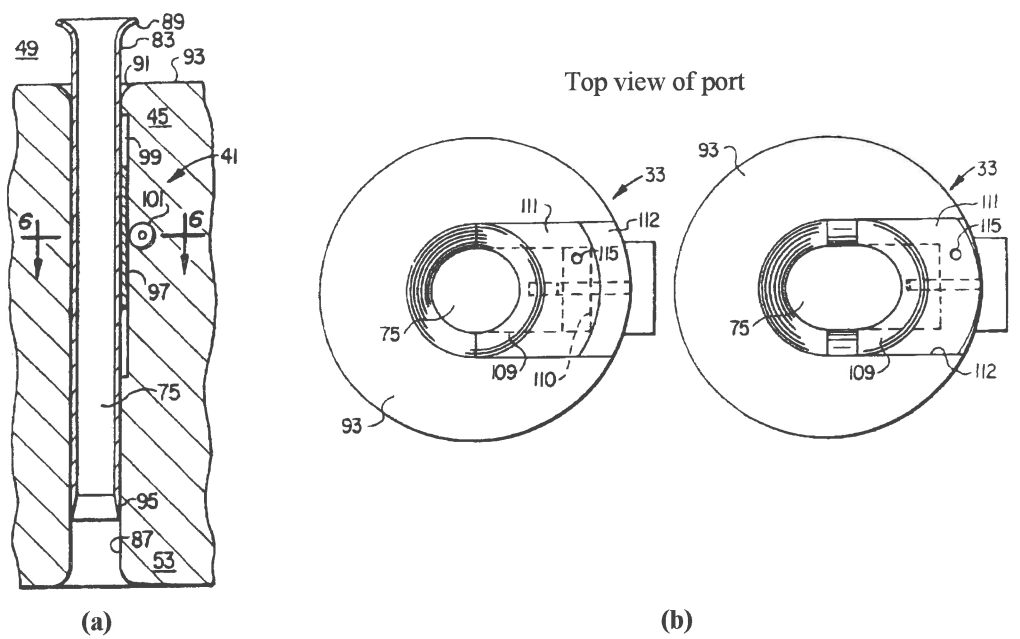

Figure 1.22 Adjustable (a) port length and (b) area (Smith & Stamps, 1998)

The fluidlastic® mount manufactured by the Lord Corporation is the only instance of a commercially available vibration absorber. Its construction was greatly simplified by keeping the port stationary and forcing the fluid through it. Furthermore it was not necessary to move the outer housing independently from the inner housing since a diaphragm was fitted at the bottom of the mount.

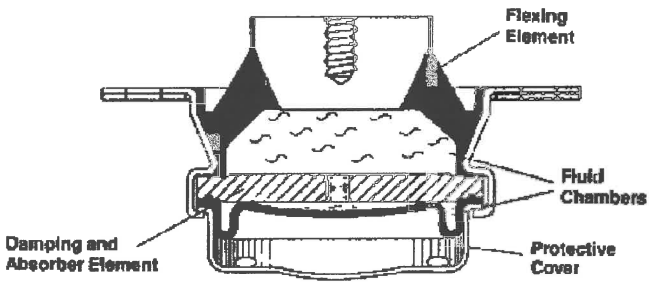

Figure 1.23 Sectional view of the fluidlastic® mount (Lord Corporation)

1.5 Objectives

The LIVE concept is the most suitable design for the attenuation of screen excitation forces. Its main advantages are the low maintenance requirements and reduced complexity. The benefit over a pendulum configuration is its linear construction without large masses vibrating through large amplitudes. The hydraulic absorber will need regular replacement due to fatigue of the metal bellows, which will make it uneconomical for this application.

The objectives of this study are to:

- Analyse the LIVE absorber using currently available techniques like finite element analysis and computational fluid dynamics.
- Design and build a LIVE type absorber. This objective's aim is to establish design guidelines and to gain experience with construction techniques specifically relating to the elastomeric spring.
- Characterise the absorber through a series of tests. The important characteristics are isolation frequency and transmissibility.
- Use the experience gained through this process to confidently predict the applicability of this absorber for a vibrating screen application.

CHAPTER 2

Mathematical model of a liquid inertia vibration absorber

2.1 Introduction

In this chapter a mathematical model of a liquid inertia vibration absorber will be developed. The absorber is similar to the LIVE concept patented by Halwes (1980) which was discussed in the previous chapter. The basic elements of the absorber are the elastomeric spring, a tuning port containing the liquid absorber mass and two liquid reservoirs. The dimensions of the reservoirs and tuning port as well as the properties of the liquid determine the response of the system. The effect of these can be found by deriving the equations of motion, which will be done in the first paragraph.

The following paragraphs will attempt to show that the damping originates from the tuning port and the elastomeric material. It will be shown that damping plays an important role in the amount of isolation that can be achieved. The complex stiffness of the elastomeric material will also be discussed.

Next the frequency response function and the transmissibility will be derived. From these the natural frequency and the frequency of isolation of the system will be determined. It will be shown which parameters will influence the frequency of isolation and the amount of isolation that can be achieved. The transmissibility will be non-dimensionalised to gain a better understanding of how optimal parameters can be found. Finally the possibility of optimising the design will be dealt with.

2.2 Equations of motion

The equations of motion will be derived for two cases. The first paragraph will deal with the basic design with square inlets. The purpose is to show how the equations are formulated and which design variables will influence the response. These equations are fairly easy to use and will be utilised for the design. Next, a more refined design using conical inlet geometry will be considered. Conical inlets will be used to reduce the amount of flow losses, but it will also influence the amount of absorber mass needed to achieve isolation at a certain frequency. The analysis of conical inlets can easily be expanded to accommodate any arbitrary inlet geometry.

2.2.1 Square inlet/outlet geometry

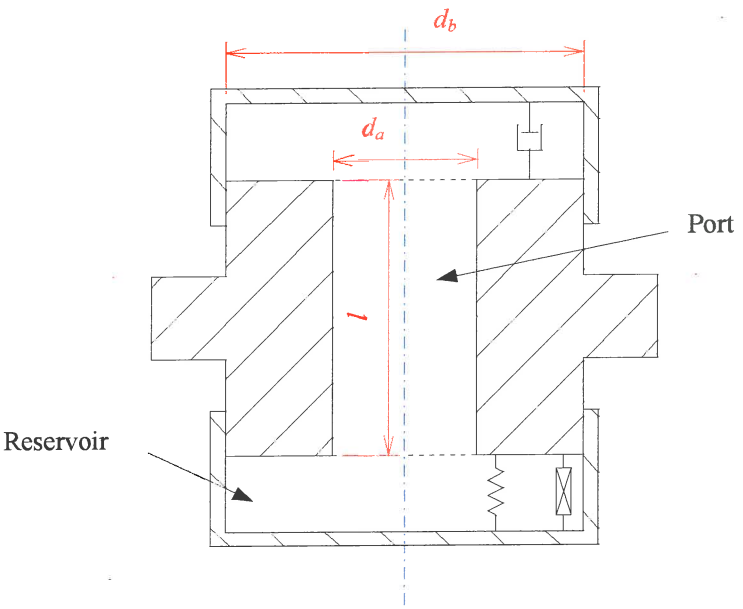

Figure 2.1 Definition of the liquid inertia system's geometry

The response of the system is governed by only 3 geometric variables (refer to figure 2.1):

- The tuning port length, l.
- The reservoir diameter, d_b. The area of the reservoir is denoted A_b.
- The port diameter, d_a. The area of the port is denoted A_a.

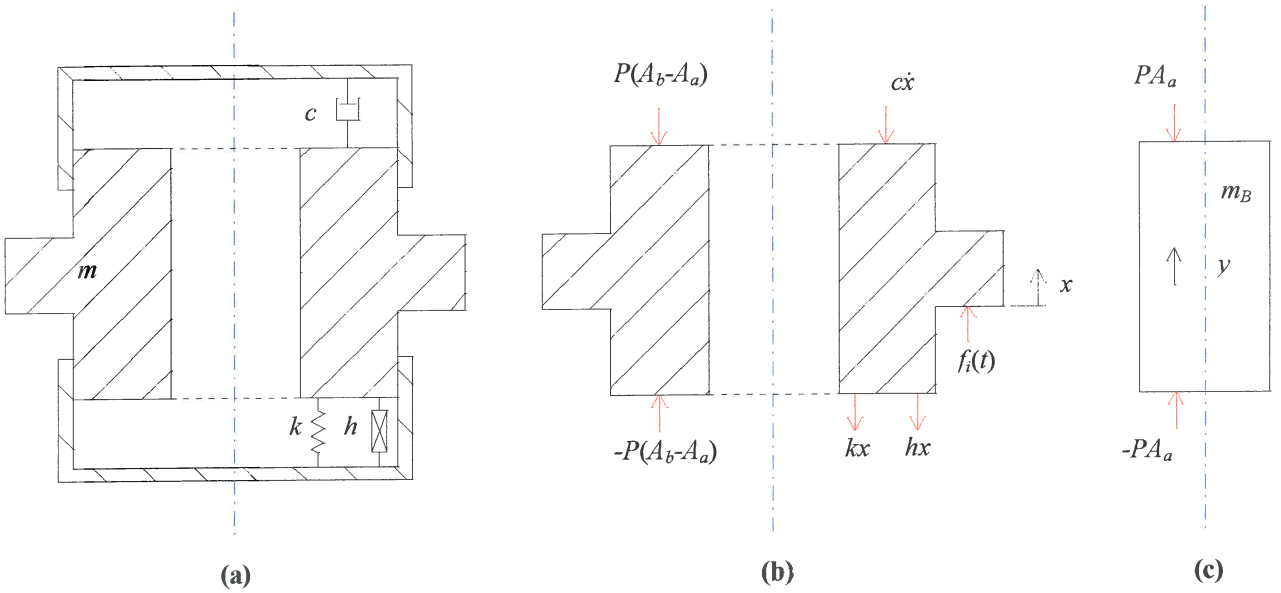

Figure 2.2 (a) Forces acting on primary system, (b) the absorber assembly, (c) forces acting on the liquid column in the tuning port

x and y denotes the displacement of the port and the liquid respectively. The relationship between $\dot{x}$ and $\dot{y}$ can be found by applying mass conservation. This relationship is called the continuity equation:

$$\begin{aligned} \dot{y}A_a &= -\dot{x}(A_b - A_a) \\ \dot{y} &= \left(1 - \frac{A_b}{A_a}\right)\dot{x} \end{aligned} \tag{2.1}$$

The force balance on the system mass (m) is:

$$m\ddot{x} = -c\dot{x} - kx - ihx - 2P(A_b - A_a) + f_i(t) \tag{2.2}$$

It is assumed that the elastomeric spring losses can be modelled using structural damping (h). The viscous damping (c) is a result of the absorber fluid losses through the tuning port.

The force balance on the absorber mass ($m_B = \rho l A_a$) is:

$$m_B\ddot{y} = -2PA_a \tag{2.3}$$

Substituting the acceleration in equation 2.3 with the conservation of mass found in equation 2.1 gives:

$$P = -\frac{m_B}{2A_a^2}(A_a - A_b)\ddot{x} \tag{2.4}$$

Using equation 2.4 the unknown pressure in equation 2.2 can be substituted to give the following single degree-of-freedom equation of motion for the system:

$$\left[m + m_B\left(1 - \frac{A_b}{A_a}\right)^2\right]\ddot{x} + c\dot{x} + k(1 + i\eta)x = f_i(t) \tag{2.5}$$

where the structural damping was written in terms of the loss factor ($h = k\eta$).

Equation 2.5 shows that the absorber mass is amplified by the area ratio and added to the system mass. The first benefit of the absorber is therefore that mass can be added to a system at relatively low cost. The second useful property of this system regards the cancellation of dynamic forces and will be shown with the derivation of the transmissibility in §2.7. Since damping plays a very important role in the amount of isolation that can be achieved, it will be discussed thoroughly.

2.2.2 Conical inlet/outlet geometry

A square inlet is very ineffective because it results in high flow losses. To reduce the amount of energy loss a smooth transition is needed. In such a port the mass and the velocity are functions of the distance from the entrance to the inlet. This paragraph will show how this effect is accounted for in the equations of motion. A formula will be derived that can be used for conical inlets, but the method can be used for any inlet geometry. The new geometry is defined in figure 2.3:

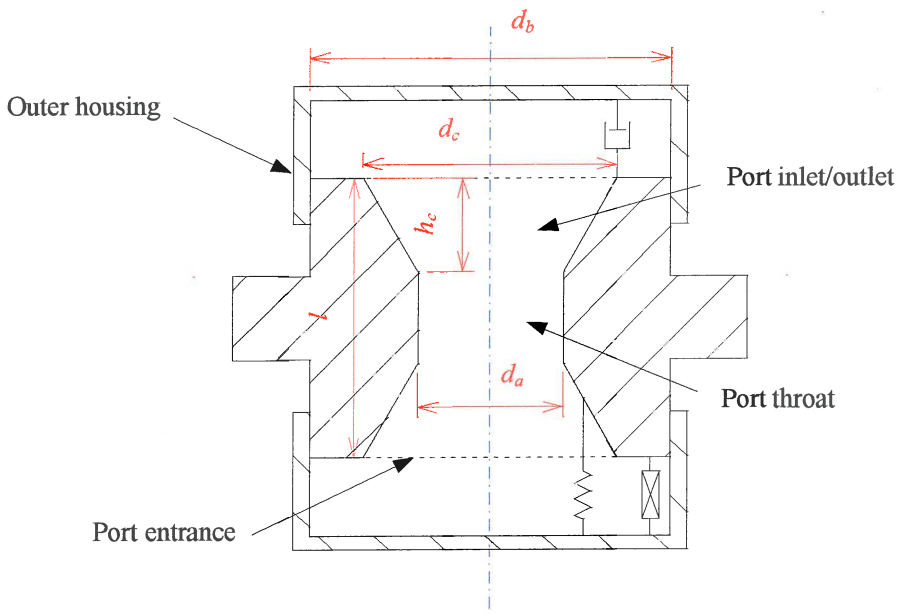

Figure 2.3 Definition of the geometry of an absorber with conical inlet/outlet

Two variables are introduced to describe the inlet geometry. They are the inlet height (h_c) and the inlet diameter (d_c). The area at the port entrance is denoted A_c.

In the previous section, the equation of motion was derived using Newton's second law of motion. For the derivation of the equation of motion in this paragraph Lagrange's equations will be used and a second degree-of-freedom (u) will be added to the system because it simplifies this analysis. Lagrange's equations are (Rao, 1990):

$$\frac{d}{dt}\left(\frac{\partial T}{\partial \dot{x}_j}\right) - \frac{\partial T}{\partial x_j} + \frac{\partial V}{\partial x_j} = Q_j^{(n)} \qquad j = 1,2,\ldots,n \qquad \textbf{(2.6)}$$

where j represents the number of degrees-of-freedom. The kinetic energy (T) is a function of mass and velocity. Both the mass and the velocity in the tuning port inlet/outlet and throat sections are functions of the geometry of the tuning port.

The following relationships are therefore needed before the kinetic energy term in Lagrange's equations can be derived:

1. The relationship between all the velocities defined by the dependent (z and y) and independent (x and u) degrees-of-freedom (figure 2.4).
2. The relationship between the inlet/outlet area and mass and the distance from the port entrance.

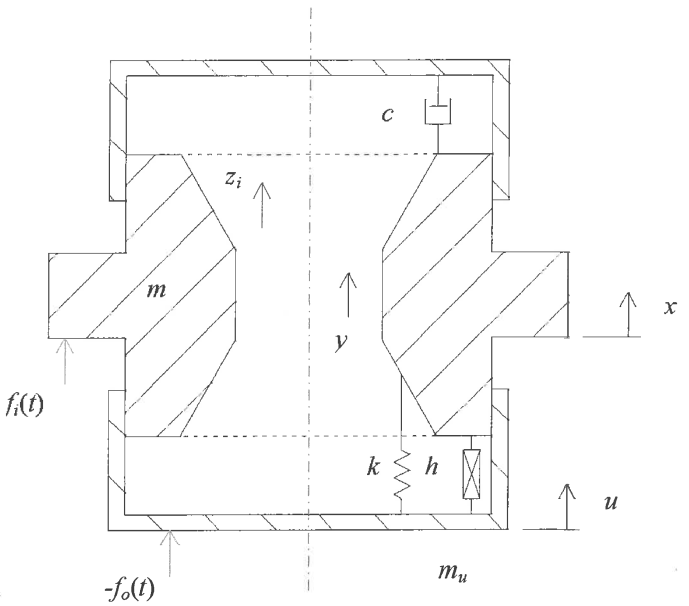

Figure 2.4 Definition of forces and displacements

The relationship between the primary system velocity ($\dot{x}$), the outer housing velocity ($\dot{u}$) and the fluid velocity in the port throat ($\dot{y}$) is given in terms of the areas:

$$-A_a\dot{y} = (A_b - A_a)\dot{x} - A_b\dot{u}$$
$$\dot{y} = \left(1 - \frac{A_b}{A_a}\right)\dot{x} + \frac{A_b}{A_a}\dot{u} \qquad (2.7)$$

The velocity in the port throat is directly related to the velocity in the inlet/outlet:

$$\dot{z} = \frac{A_a}{A_i}\dot{y} \qquad (2.8)$$

From these two equations the velocity in the inlet/outlet can be found in terms of the primary system and outer housing velocities:

$$\dot{z} = \left(\frac{A_a - A_b}{A_i}\right)\dot{x} + \frac{A_b}{A_i}\dot{u} \qquad (2.9)$$

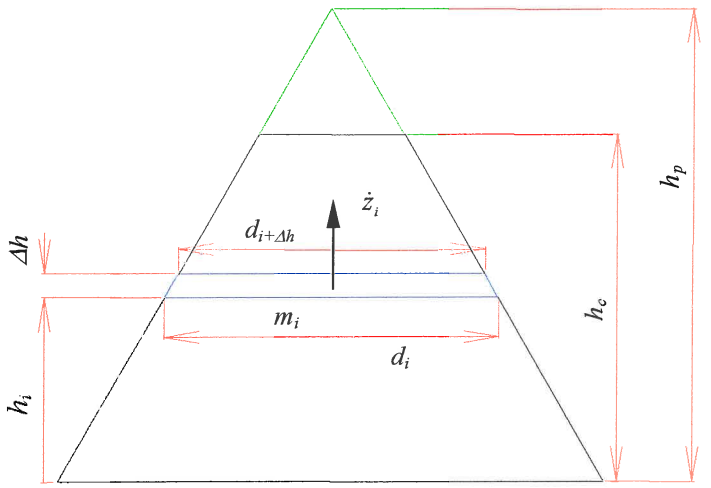

Figure 2.5 Inlet geometry definitions

The mass m_i at a distance h_i from the entrance to the port can be written in terms of the geometry and the density:

$$m_i = \frac{1}{3}\rho\frac{A_i}{(h_p - h_i)^2}\left[3\Delta h(h_p - h_i)^2 - 3\Delta h^2(h_p - h_i) + \Delta h^3\right] \tag{2.10}$$

For $\Delta h \rightarrow 0$ the higher order terms can be neglected and the equation reduces to the mass of a cylinder with height Δh:

$$m_i = \rho A_i \Delta h \tag{2.11}$$

The area is a function of the distance from the entrance to the inlet and the height of the cone defined by the inlet geometry (h_p):

$$A_i = \frac{A_c}{h_p^2}(h_p - h_i)^2 \tag{2.12}$$

The distance h_p can be expressed as a function of the basic geometric variables as follows:

$$h_p = \frac{d_c h_c}{d_c - d_a} \tag{2.13}$$

The total kinetic energy is the sum of the contribution of the primary system (m), the absorber mass in the throat of the port (m_p), the liquid in the inlet/outlet and the outer housing mass (m_u):

$$T = \frac{1}{2}\left(m\dot{x}^2 + m_p\dot{y}^2 + 2\sum m_i\dot{z}_i^2 + m_u\dot{u}^2\right) \tag{2.14}$$

After substituting the velocity values described by equation 2.7 and 2.9 the kinetic energy becomes:

$$T = \frac{1}{2}\left\{ m\dot{x} + m_p\left[\left(1-\frac{A_b}{A_a}\right)\dot{x} + \frac{A_b}{A_a}\dot{u}\right]^2 + 2\sum_{i=1}^{n} m_i\left[\left(1-\frac{A_b}{A_i}\right)\dot{x} + \frac{A_b}{A_i}\dot{u}\right]^2 + m_u\dot{u}^2 \right\} \tag{2.15}$$

From equation 2.15 the kinetic energy terms in Lagrange's equations can be derived:

$$\frac{d}{dt}\left(\frac{\partial T}{\partial \dot{x}}\right) = \left[m + m_p\left(1-\frac{A_b}{A_a}\right)^2 + 2(A_a - A_b)^2\sum_{i=1}^{n}\frac{m_i}{A_i^2}\right]\ddot{x} + \left[m_p\left(1-\frac{A_b}{A_a}\right)\frac{A_b}{A_a} + 2(A_a - A_b)A_b\sum_{i=1}^{n}\frac{m_i}{A_i^2}\right]\ddot{u} \tag{2.16}$$

$$\frac{d}{dt}\left(\frac{\partial T}{\partial \dot{u}}\right) = \left[m_p\left(1-\frac{A_b}{A_a}\right)\frac{A_b}{A_a} + 2(A_a - A_b)A_b\sum_{i=1}^{n}\frac{m_i}{A_i^2}\right]\ddot{x} + \left[m_p\left(\frac{A_b}{A_a}\right)^2 + 2A_b^2\sum_{i=1}^{n}\frac{m_i}{A_i^2} + m_u\right]\ddot{u} \tag{2.17}$$

The elastic energy is simply:

$$V = \frac{1}{2}k(x-u)^2 \tag{2.18}$$

The elastic energy terms in Lagrange's equations are:

$$\frac{\partial V}{\partial x} = kx - ku \tag{2.19}$$

$$\frac{\partial V}{\partial u} = -kx + ku \tag{2.20}$$

The damping and external forces are represented by Q_j^n. The complete equation of motion is:

$$[M]\{\ddot{x}\} + [C]\{\dot{x}\} + ([K] + i[H])\{x\} = \{f\} \tag{2.21}$$

If displacement u is set to zero then the force acting on the outer housing becomes the reaction force transmitted to the ground. The system simplifies to a single degree-of-freedom and its motion is described by the first equation in the set given by equation 2.21.

$$\left[m + m_p\left(1-\frac{A_b}{A_a}\right)^2 + 2(A_a - A_b)^2\sum_{i=1}^{n}\frac{m_i}{A_i^2}\right]\ddot{x} + c\dot{x} + k(1+i\eta)x = f_i(t) \tag{2.22}$$

This equation can be applied to any inlet geometry provided that A_i is known (m_i is dependent on A_i). If the area and the mass found in equation 2.11 and 2.12 are substituted and the sum is replaced by an integral the equation of motion becomes:

$$\left[m + \rho A_a(l-2h_c)\left(1-\frac{A_b}{A_a}\right)^2 + 2\rho\frac{A_a^2 h_p^2}{A_c}\left(1-\frac{A_b}{A_a}\right)^2\int_0^{h_c}\frac{1}{(h_p-h)^2}dh\right]\ddot{x} + c\dot{x} + k(1+i\eta)x = f_i(t) \tag{2.23}$$

Evaluating the integral leaves:

$$\left\{m+\rho A_a\left[l-2h_c+2\frac{A_a}{A_c}\left(\frac{h_p^2}{h_p-h_c}-h_p\right)\right]\left(1-\frac{A_b}{A_a}\right)^2\right\}\ddot{x}+c\dot{x}+k(1+i\eta)x=f_i(t) \qquad (2.24)$$

The force acting on the ground can be found by evaluating the second equation in the set given by equation 2.21.

$$\rho\left[l-2h_c+2\frac{A_a}{A_c}\left(\frac{h_p^2}{h_p-h_c}-h_p\right)\right]\left(1-\frac{A_b}{A_a}\right)A_b\ddot{x}-c\dot{x}-k(1+i\eta)x=-f_o(t) \qquad (2.25)$$

2.3 Viscous damping

In viscous damping, the damping force is proportional to the velocity (Rao, 1990). The forces acting on the tuning port at constant velocity is the shear force on the port wall (F_τ) and the pressure difference across the port (Δp_T). The total pressure loss consists of the pressure loss across the inlet (Δp_i), the outlet (Δp_o), and the port (Δp_w). The shear force acting in the axial direction is a function of the shear stress (τ_w) acting on the port area.

The objective of this paragraph is to find the damping coefficient as a function of the velocity of the tuning port. All the equations in the literature are however given as a function of the velocity of the liquid inside the port. The following continuity equation relates the average velocity of the fluid in the port (V) and the velocity of the port ($\dot{x}$):

$$\begin{aligned} V &= |\dot{y}| \\ &= \left(\frac{d_b^2}{d_a^2}-1\right)|\dot{x}| \end{aligned} \qquad (2.26)$$

The pressure drop across the port and the shear stress on the port wall is dependent on whether the flow is turbulent or laminar. The flow is considered to be laminar for $Re_d < 2300$. The expression for laminar shear stress is (White, 1988):

$$\begin{aligned} \tau_w^l &= \frac{\mu u_{\max}}{d_a} \\ &= \frac{2\mu V}{d_a} \end{aligned} \qquad (2.27)$$

The average velocity (V) for laminar flow is $\frac{1}{2}u_{max}$ and μ is the absolute viscosity. The expression for turbulent shear stress is (White, 1991):

$$\tau_w^t = 0.0396\rho^{3/4}V^{7/4}\mu^{1/4}d_a^{-1/4} \qquad (2.28)$$

According to White (1991) the laminar pressure drop is:

$$\Delta p_w^l = \frac{32\mu l V}{d_a^2} \tag{2.29}$$

and the turbulent pressure drop is:

$$\Delta p_w^t \approx 0.158\rho^{3/4}V^{7/4}\mu^{1/4}d_a^{-5/4} \tag{2.30}$$

The pressure drop across the inlet and the outlet is expressed in terms of loss coefficients. The relationship between the loss coefficient and the head loss is:

$$K = \frac{h_m}{V^2/2g} \tag{2.31}$$

The loss coefficient is a function of the inlet or outlet geometry. It is important to note that the port oscillates and the inlet will also act as an outlet and *vice versa*. It is therefore not advisable to design them with different geometries. The loss coefficients will be discussed using available theoretical and empirical coefficients. Since none of these exactly represent the theoretical model it will be compared with computational fluid dynamics (CFD) results. The three possibilities are:

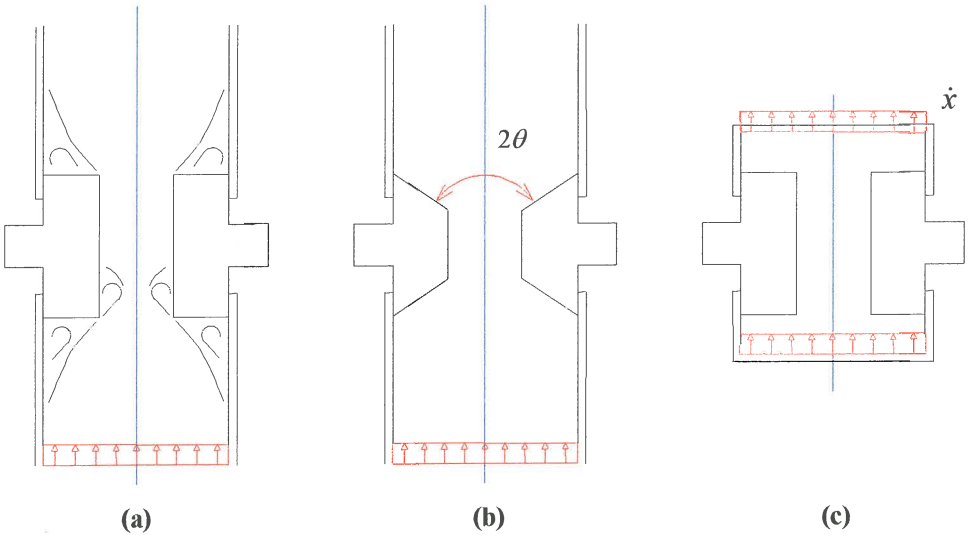

Figure 2.6 Different inlet/outlet configurations with the radially constant velocity boundary condition shown (a) infinite boundary, (b) diffuser, (c) realistic boundary

The solutions for configurations (a) and (b) have been published by White (1988). For a realistic boundary that is very close to the inlet, a solution had to be found using CFD.

2.3.1 Infinite boundary

The loss coefficient for a sudden contraction (at the inlet) is (White, 1988):

$$K_i \approx 0.42\left(1-\frac{d_a^2}{d_b^2}\right) \tag{2.32}$$

The loss coefficient for a sudden expansion (at the outlet) is expressed as:

$$K_o = \left(1-\frac{d_a^2}{d_b^2}\right)^2 \tag{2.33}$$

The head loss is related to the pressure drop by:

$$h_m = \frac{\Delta p}{\rho g} \tag{2.34}$$

The inlet pressure drop is therefore:

$$\Delta p_i \approx 0.42\left(1-\frac{d_a^2}{d_b^2}\right)\rho\frac{V^2}{2} \tag{2.35}$$

and the outlet pressure drop is:

$$\Delta p_o = \left(1-\frac{d_a^2}{d_b^2}\right)^2 \rho\frac{V^2}{2} \tag{2.36}$$

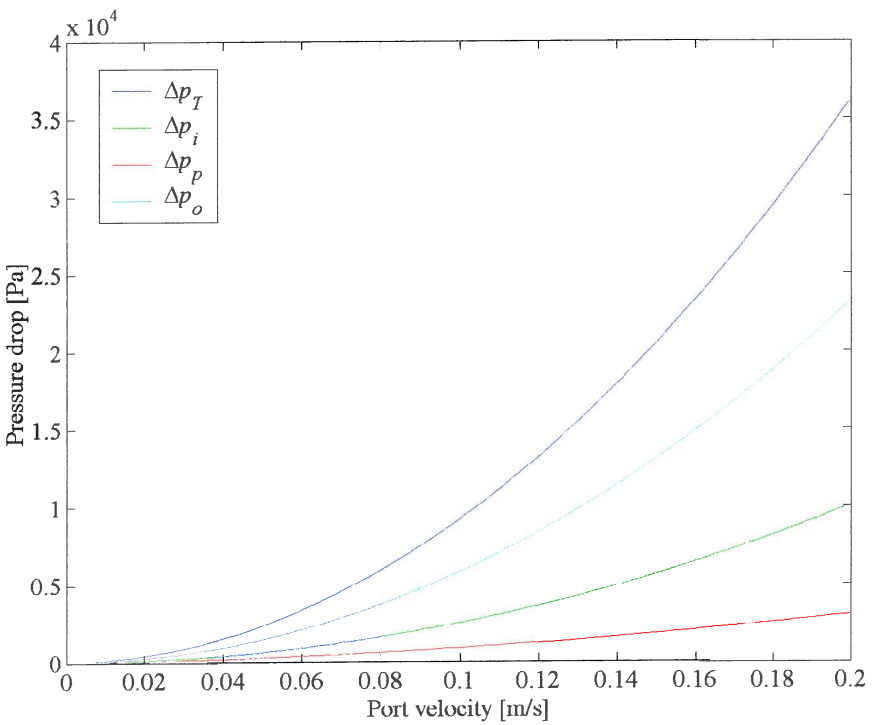

Figure 2.7 Pressure drop across the inlet, port and the outlet as a function of the port velocity ($\dot{x}$)

The force acting on the tuning port can be found in terms of the pressure difference and the shear stress on the port wall:

$$F_c = \Delta p_T (A_b - A_a) + \tau_w \pi d_a l \tag{2.37}$$

The nonlinear damping coefficient is therefore:

$$c = \frac{F_c}{\dot{x}} \tag{2.38}$$

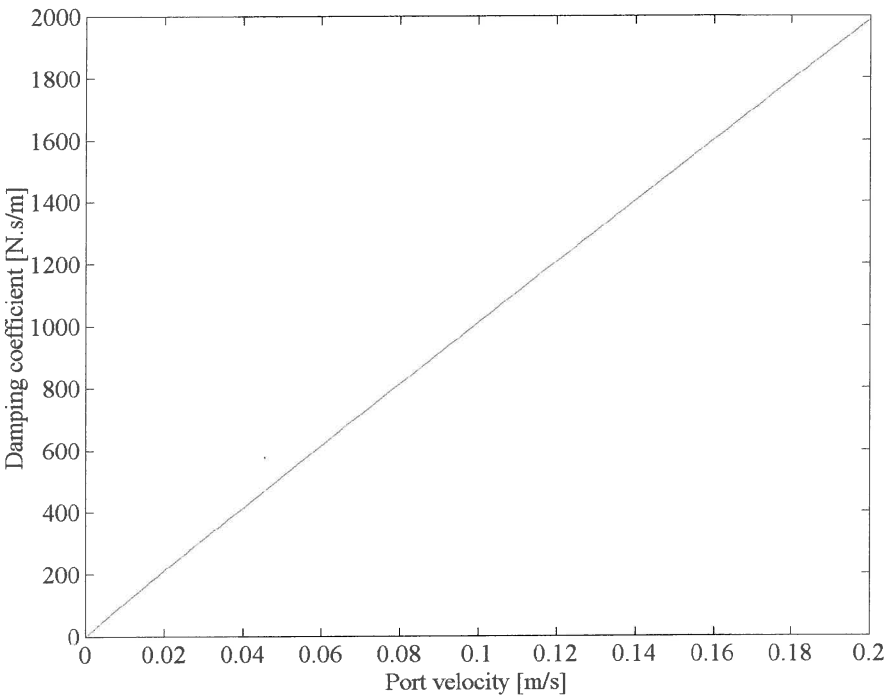

Figure 2.8 Damping as a function of the port velocity

The infinite boundary assumption does not accurately describe the flow conditions of the system. The following can however be learnt from the above analysis:

- The flow in the port will be turbulent.
- The turbulent flow loss in the port is more dependent on density than on viscosity.
- Small port diameters and large port velocities should be avoided. Large port velocities are a result of high area ratios (refer to equation 2.26).
- The inlet and outlet losses dominate the port losses.

From the above it is clear that the inlet and outlet geometry should be optimised to ensure low losses. The following paragraph will discuss how diffusers can be used in this regard.

2.3.2 Diffusers

A diffuser is a gradual conical expansion. The loss coefficient is given in terms of the pressure recovery coefficient:

$$C_p = \frac{p_2 - p_1}{\frac{1}{2}\rho V_1^2} \tag{2.39}$$

p_2 is the downstream pressure and p_1 the pressure in the port. The outlet loss coefficient is:

$$K_o = 1 - \frac{d_1^4}{d_2^4} - C_p \tag{2.40}$$

C_p values are determined experimentally. According to White (1988) the minimum value for K_o occurs at $2\theta = 5°$. For cone angles between 40° and 60° the loss becomes larger than for a sudden expansion. The inlet loss coefficient is very small as can be seen from the following experimental values:

Table 2.1 The inlet loss coefficient (White, 1988)

Diffuser angle (2θ) [deg]	Inlet loss coeffcient K_i
30	0.02
45	0.04
60	0.07

From the above analysis of diffusers it seems that diffusers can be used to reduce the amount of flow losses at the inlet and the outlet. The small angle required might make it impractical since it will require a very long port.

2.3.3 Realistic boundary

The boundary condition as shown in figure 2.6(c) is the result of the constraint put on the flow by the moving primary system. The flow next to the wall should have the same velocity as the wall. Since the boundary is very close to the inlet and outlet the losses are larger than that shown in §2.3.1. The flow through the port was analysed using STAR-CD, a commercial CFD package. The total pressure drop was calculated. The resultant force in the direction of the flow was also calculated. This includes the shear force on the port wall as well as the force resulting from the total pressure drop. The calculations were done for different inlet velocities. The inlet boundary velocity is the equal to the primary system velocity.

$$|\dot{x}| = \omega X \tag{2.41}$$

The relative pressure is calculated by the CFD program. p_i and p_o are the average pressures at the inlet and outlet respectively. The pressure loss is:

$$\Delta p_T = p_i - p_o \tag{2.42}$$

The pressure loss is shown in figure 2.9.

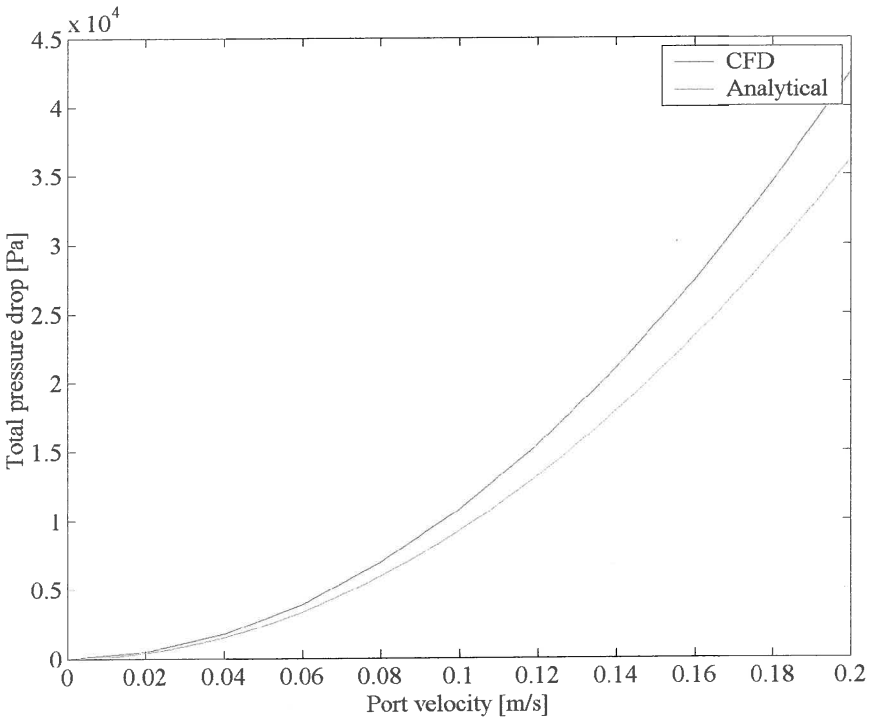

Figure 2.9 The total pressure drop across the port, as calculated using CFD (blue) and the sudden contraction and expansion analytical equations (green), as a function of port velocity

The pressure loss calculated using the two methods shows good comparison. The pressure loss calculated with the CFD method is slightly higher because of the effect the proximity of the boundary to the port entrance has on the inlet and outlet pressure loss. It seems as if the loss can be minimised by increasing the distance between the boundary and the port. This will of course affect the total height of the absorber, which will probably be limited by the available space and economics.

The damping coefficient is shown in figure 2.10. The coefficient is a linear function of frequency.

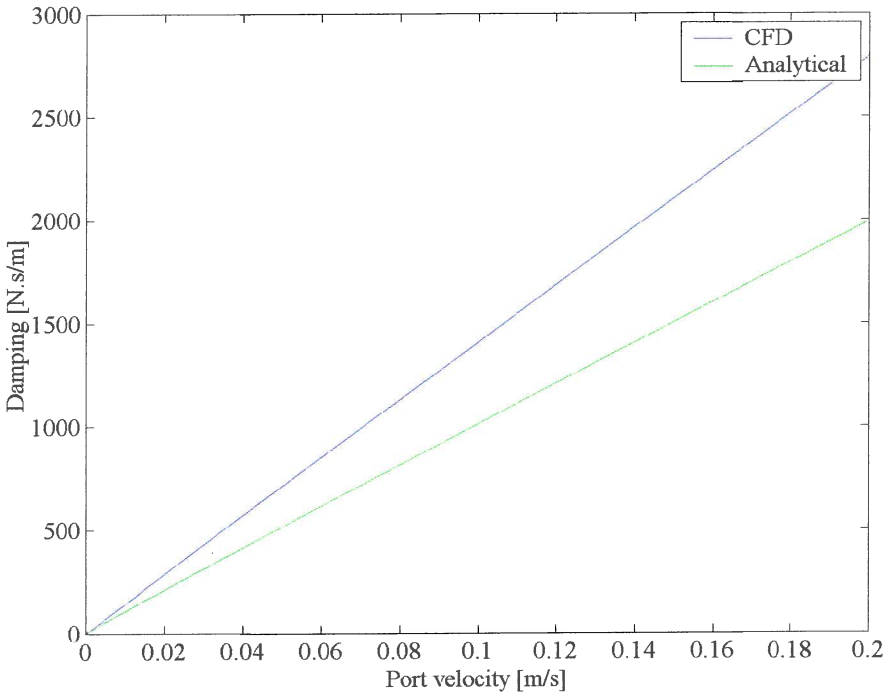

Figure 2.10 The damping coefficient, as calculated using CFD and the sudden contraction and expansion analytical equations, as a function of port velocity

2.4 Material damping

When materials are deformed, energy is absorbed and dissipated by the material. The material damping is given in terms of the loss factor. The loss factor is defined as the ratio of the loss and storage moduli (Garibaldi *et al.*, 1996):

$$\eta = \tan(\theta) = \frac{\text{Loss modulus } (E'')}{\text{Storage modulus } (E')} \tag{2.43}$$

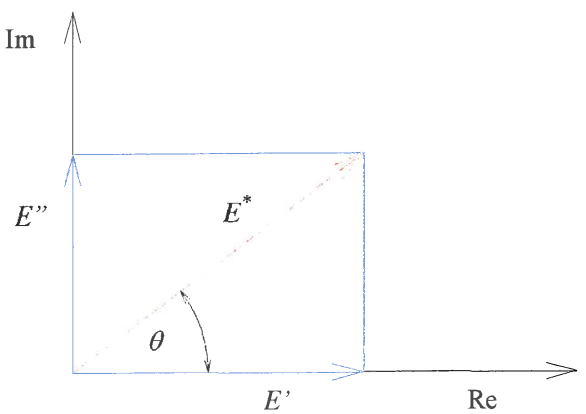

Figure 2.11 The definition of the loss factor

The loss factor must be measured experimentally and published values do exist for various kinds of elastomers (Nashif *et al.*, 1985).

2.5 Stiffness

The stiffness (k) is a function of the real part of the complex modulus in figure 2.11, and the geometry:

$$E^* = E' + iE'' \tag{2.44}$$

The stiffness of elastomeric compounds is a function of the strain rate and therefore of frequency (Davey *et al.*, 1964). For the purposes of this chapter the stiffness will assumed to be constant.

2.6 Frequency response function

Equation 2.5 can be transformed to the frequency domain by substituting the harmonic response and its derivatives, which results from harmonic excitation:

$$x(t) = Xe^{i\omega t} \tag{2.45}$$

$$\dot{x}(t) = i\omega Xe^{i\omega t} \tag{2.46}$$

$$\ddot{x}(t) = -\omega^2 Xe^{i\omega t} \tag{2.47}$$

$$f_i(t) = F_i e^{i\omega t} \tag{2.48}$$

$$\frac{X}{F_i} = \frac{1}{k(1+i\eta)+i\omega c-\omega^2\left[m+m_B\left(1-\frac{A_b}{A_a}\right)^2\right]} \tag{2.49}$$

The undamped natural frequency of this system is:

$$\omega_n = \sqrt{\frac{k}{m+m_B\left(1-\frac{A_b}{A_a}\right)^2}} \tag{2.50}$$

The normalised response and phase angle are:

$$\frac{X}{\delta_{st}} = \frac{1}{\left\{\left[1-\left(\frac{\omega}{\omega_n}\right)^2\right]^2 + \left[2\zeta\frac{\omega}{\omega_n}+\eta\right]^2\right\}^{\frac{1}{2}}} \tag{2.51}$$

$$\phi = \tan^{-1}\left\{\frac{2\zeta\frac{\omega}{\omega_n}}{1-\left(\frac{\omega}{\omega_n}\right)^2}\right\} \tag{2.52}$$

The ratio of the natural frequency of the system with (ω_n) and without (ω_n') an absorber is:

$$G_n = \frac{\omega_n}{\omega_n'} = \sqrt{\frac{m}{m+m_B\left(1-\frac{A_b}{A_a}\right)^2}} \tag{2.53}$$

Figure 2.12 shows the effect of the absorber on the system response for a certain frequency ratio (G_n). As mass is added to the system with the vibration absorber the natural frequency decreases. G_n is of course always less than one.

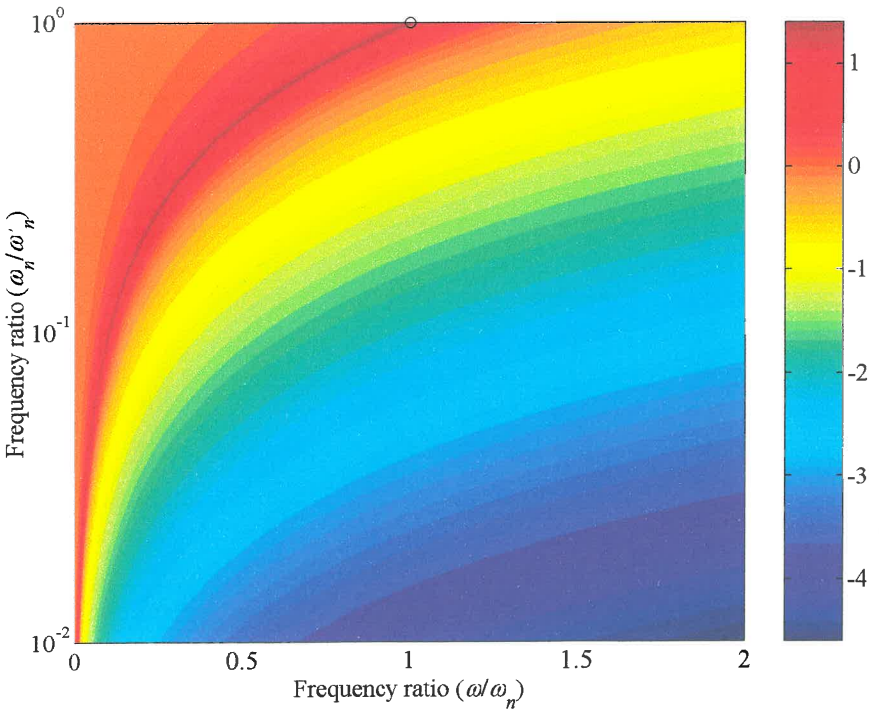

Figure 2.12 The log response of the system ($\log|X/\delta_{st}|$) as a function of the frequency ratio indicates the shift in natural frequency as mass is added to the system with $\zeta = 0.01$ and $\eta = 0.01$

2.6.1 FRF of a system with a conical inlet/outlet geometry

The FRF for a system with a conical inlet/outlet is:

$$\frac{X}{F_i} = \frac{1}{k(1+i\eta)+i\omega c-\omega^2\left\{m+\rho A_a\left[l-2h_c+2\frac{A_a}{A_c}\left(\frac{h_p^2}{h_p-h_c}-h_p\right)\right]\left[1-\frac{A_b}{A_a}\right]^2\right\}} \tag{2.54}$$

The inlet reduces the effective absorber mass. If the absorber mass terms in equation 2.54 is compared to that in equation 2.5 the following results:

$$M_r = \frac{l-2h_c+2\frac{A_a}{A_c}\left(\frac{h_p^2}{h_p-h_c}-h_p\right)}{l} \tag{2.55}$$

Equation 2.55 is plotted in figure 2.13 to illustrate the effect of the inlet dimensions (h_c and d_c) on the absorber mass ratio. The effective absorber mass can be significantly reduced with the addition of conical inlet/outlet.

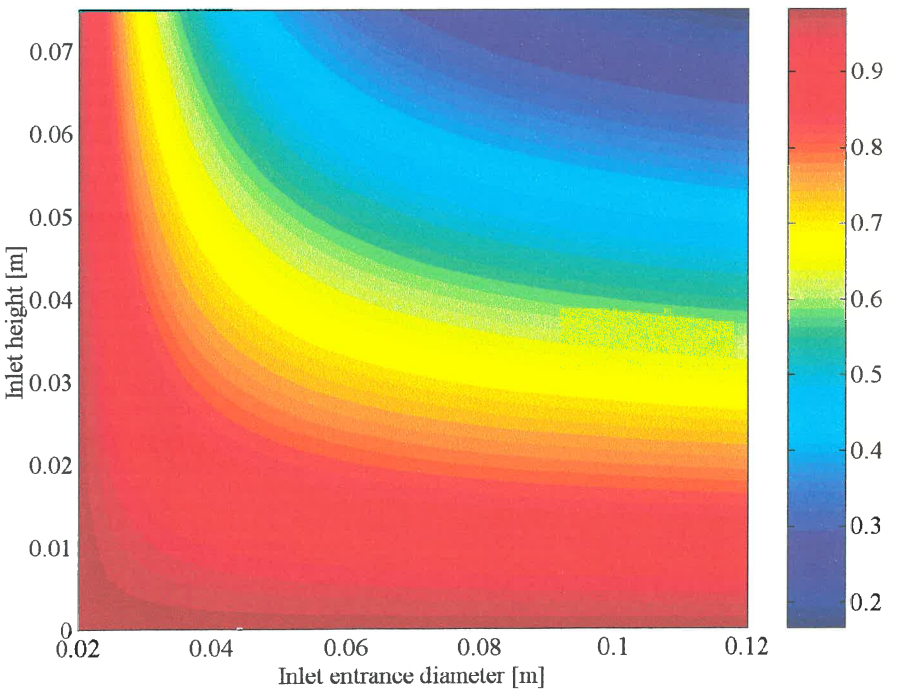

Figure 2.13 Absorber mass ratio as a function of inlet diameter (d_c) and height (h_c)

2.7 Transmissibility

The transmissibility is defined as the force amplitude ratio of the force transmitted to the ground (F_o) and the applied force (F_i).

The applied force can be derived from equation 2.49:

$$F_i = \left\{ k(1+i\eta) + i\omega c - \omega^2 \left[m + m_B \left(1 - \frac{A_b}{A_a} \right)^2 \right] \right\} X \tag{2.56}$$

The force resulting from the pressure difference in the reservoirs is (figure 2.2):

$$F_p = 2PA_b \tag{2.57}$$

The peak pressure is (equation 2.4):

$$P = \frac{m_B}{2A_a} \left(1 - \frac{A_b}{A_a} \right) \omega^2 X \tag{2.58}$$

The pressure in equation 2.57 can now be eliminated:

$$F_p = m_B \left(1 - \frac{A_b}{A_a} \right) \frac{A_b}{A_a} \omega^2 X \tag{2.59}$$

The force acting on the ground is a combination of the pressure, the spring stiffness and structural damping as well as the viscous damping. The reaction force on the ground is therefore:

$$F_o = \left[k(1+i\eta) + i\omega c + \omega^2 m_B \left(1 - \frac{A_b}{A_a} \right) \frac{A_b}{A_a} \right] X \tag{2.60}$$

The transmissibility is given by eliminating X in equations 2.56 and 2.60:

$$\frac{F_o}{F_i} = \frac{k(1+i\eta) + i\omega c + \omega^2 m_B \left(1 - \frac{A_b}{A_a} \right) \frac{A_b}{A_a}}{k(1+i\eta) + i\omega c - \omega^2 \left[m + m_B \left(1 - \frac{A_b}{A_a} \right)^2 \right]} \tag{2.61}$$

The objective of the absorber is to minimise the force transmitted to the ground. This can be achieved by choosing the parameters in equation 2.61 correctly. The following paragraphs will show how this is accomplished.

2.7.1 Undamped frequency of isolation

The transmitted force in equation 2.60 can be rearranged in real and imaginary parts:

$$F_o = \left[k + \omega^2 m_B \left(1 - \frac{A_b}{A_a} \right) \frac{A_b}{A_a} + i(\omega c + k\eta) \right] X \tag{2.62}$$

The real part of equation 2.62 can be zero for a specific frequency. This frequency is called the isolation frequency and is:

$$\omega_a = \sqrt{\frac{-k}{m_B \left(1 - \frac{A_b}{A_a} \right) \frac{A_b}{A_a}}} \tag{2.63}$$

In the literature this frequency is often termed the anti-resonant frequency. Equation 2.63 is exactly the same as that found by Halwes (1980). Halwes derived this frequency for an undamped two degree-of-freedom system and defined the transmissibility in terms of displacements. Since anti-resonance for an undamped system is defined as a point of no response to excitation (Maia *et al.*, 1998) and since the absorber discussed here does not aim to do that, the term isolation frequency will be used.

It is important to note that isolation frequency is independent of the system mass. This is an extremely attractive property since a changing system mass, as may be the case for a screen carrying different loads, will not affect the isolation frequency. The imaginary part can never be zero. Ensuring the lowest possible structural and viscous damping can however minimise the force transmitted to the ground.

2.7.2 Damped frequency of maximum and minimum transmissibility

The frequency of minimum transmissibility (isolation) for the damped case is more difficult to obtain. In this case the force transmitted to the ground is not zero at the isolation frequency, but equal to the damping force. Increasing the value of the denominator in equation 2.61 can now be used to minimise the transmissibility. The frequency of isolation can be found by differentiating the absolute value of the transmissibility with respect to frequency:

$$\frac{\partial}{\partial \omega} \left\{ \frac{\left(k + \omega^2 m_B \left(1 - \frac{A_b}{A_a} \right) \frac{A_b}{A_a} \right)^2 + (\omega c + k\eta)^2}{\left(k - \omega^2 \left[m + m_B \left(1 - \frac{A_b}{A_a} \right)^2 \right] \right)^2 + (\omega c + k\eta)^2} \right\}^{\frac{1}{2}} = 0 \tag{2.64}$$

By rewriting this equation and assigning the numerator $f(\omega)$ and the denominator $g(\omega)$ it can be differentiated as follows:

$$\frac{\partial}{\partial\omega}\left(\frac{F_o}{F_i}\right)=\frac{\partial}{\partial\omega}\left(\left\{\frac{f(\omega)}{g(\omega)}\right\}^{\frac{1}{2}}\right)=\frac{1}{2}\left(\frac{f(\omega)}{g(\omega)}\right)^{-\frac{1}{2}}\frac{f'(\omega)g(\omega)-f(\omega)g'(\omega)}{[g(\omega)]^2}=0$$

with

$$\begin{aligned}
f(\omega)&=\left(k+\omega^2 m_B\left(1-\frac{A_b}{A_a}\right)\frac{A_b}{A_a}\right)^2+(\omega c+k\eta)^2\\
f'(\omega)&=4\omega m_B\left(k+\omega^2 m_B\left(1-\frac{A_b}{A_a}\right)\frac{A_b}{A_a}\right)\left(1-\frac{A_b}{A_a}\right)\frac{A_b}{A_a}+2c(\omega c+k\eta)\\
g(\omega)&=\left(k-\omega^2\left[m+m_B\left(1-\frac{A_b}{A_a}\right)^2\right]\right)^2+(\omega c+k\eta)^2\\
g'(\omega)&=4\omega\left(k-\omega^2\left[m+m_B\left(1-\frac{A_b}{A_a}\right)^2\right]\right)\left[m+m_B\left(1-\frac{A_b}{A_a}\right)^2\right]+2c(\omega c+k\eta)
\end{aligned}\qquad \textbf{(2.65)}$$

This leads to one of the following:

$$\left(\frac{f(\omega)}{g(\omega)}\right)^{-\frac{1}{2}}=0 \qquad \textbf{(2.66)}$$

or

$$f'(\omega)g(\omega)-f(\omega)g'(\omega)=0$$

The first term can never be zero. The second term yields five roots of which one is zero, two are negative and two positive. The positive roots correspond to the frequencies of maximum and minimum transmissibility. The importance of this analysis is that the isolation frequency is no longer independent of the system mass. It is also dependent on damping, which could lead to considerable design difficulties. For the undamped case it was possible to choose a stiffness coefficient, absorber mass and port area and then calculate the reservoir area for the frequency that needs to be isolated. This method is no longer possible due to the complexity of equation 2.61. A possible solution is to solve the equation numerically.

2.7.3 Non-dimensional transmissibility

By substituting the variables in equation 2.61 with the definitions in equations 1.5 to 1.7 the non-dimensional transmissibility can now be written in terms of the undamped resonance and isolation frequencies:

$$|T_r| = \left\{ \frac{\left[1-\left(\frac{\omega}{\omega_a}\right)^2\right]^2 + \left[2\zeta\frac{\omega}{\omega_n}+\eta\right]^2}{\left[1-\left(\frac{\omega}{\omega_n}\right)^2\right]^2 + \left[2\zeta\frac{\omega}{\omega_n}+\eta\right]^2} \right\}^{\frac{1}{2}} \tag{2.67}$$

The phase angle is:

$$\phi = \tan^{-1}\left\{\frac{2\zeta\frac{\omega}{\omega_n}+\eta}{1-\left(\frac{\omega}{\omega_a}\right)^2}\right\} - \tan^{-1}\left\{\frac{2\zeta\frac{\omega}{\omega_n}+\eta}{1-\left(\frac{\omega}{\omega_n}\right)^2}\right\} \tag{2.68}$$

By choosing $\omega_a = 1$ and $\omega_n = 0.5$ the following figures could be plotted showing the influence of viscous and structural damping. The figures clearly indicate the importance of low damping for good isolation.

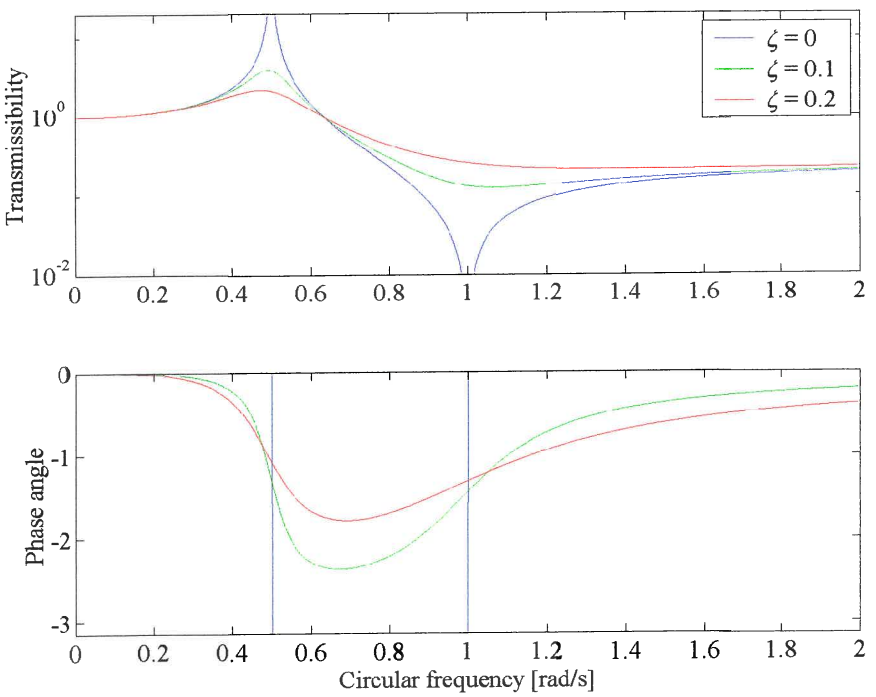

Figure 2.14 Transmissibility as a function of damping ratio with $\omega_n = 0.5$ and $\omega_a = 1$

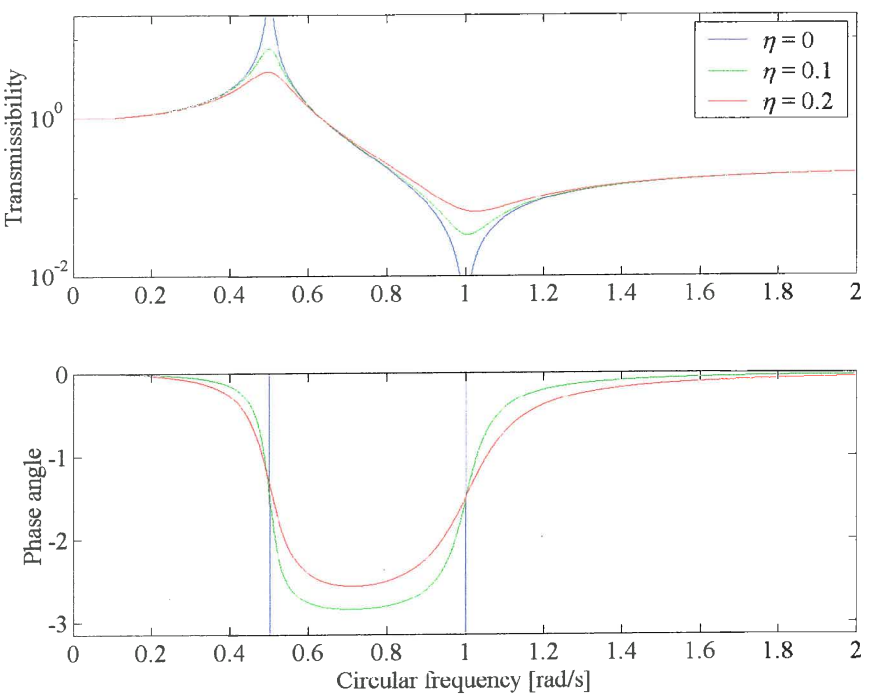

Figure 2.15 Transmissibility as a function of loss factor with $\omega_n = 0.5$ and $\omega_a = 1$

It is also important to study the effect of the frequency ratio on the amount of isolation achieved. The frequency ratio is defined as:

$$G_a = \frac{\omega_n}{\omega_a} = \sqrt{\frac{m_B\left(\frac{A_b}{A_a} - 1\right)\frac{A_b}{A_a}}{m + m_B\left(\frac{A_b}{A_a} - 1\right)^2}} \tag{2.69}$$

Figure 2.16 shows two regions of isolation at the chosen isolation frequency $\omega_a = 1$. For a frequency ratio less than one the frequency of maximum transmissibility appears before the isolation frequency. It is not feasible to design in the region where the frequency ratio is more than one. This will require a very high absorber mass (m_B) and a high area ratio. Additionally the amount of isolation will be small, the bandwidth rather narrow and high frequencies will be amplified. If the system mass is small in comparison with the absorber mass equation 2.69 reduces to:

$$G_a = \sqrt{\frac{\frac{A_b}{A_a}}{\frac{A_b}{A_a} - 1}} \tag{2.70}$$

Equation 2.70 is always greater than one for area ratios larger than one. This shows that the system mass must be large in comparison with the absorber mass to achieve good isolation.

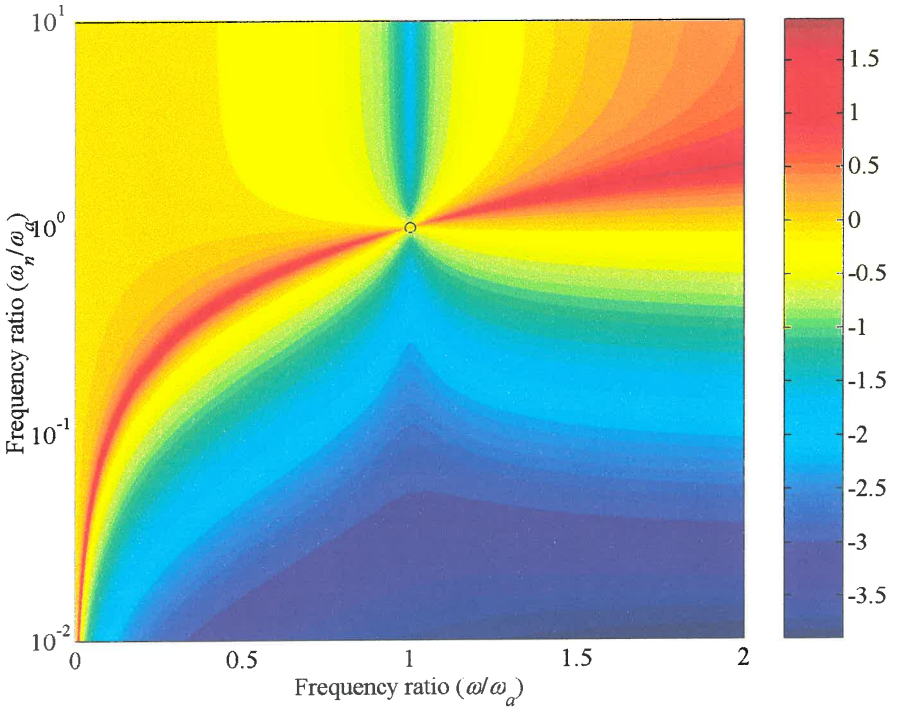

Figure 2.16 Log transmissibility ($\log|T_r|$) as a function frequency ratio (G_a) and circular frequency (ω/ω_a) with $\zeta = 0.01$ and $\eta = 0.01$ showing the isolation frequency $\omega_a = 1$

It is useful to compare the transmissibility before and after the addition of the absorber. The transmissibility without an absorber is:

$$|T_r| = \left\{ \frac{1 + \left[2\zeta \frac{\omega}{\omega_n} + \eta \right]^2}{\left[1 - \left(\frac{\omega}{\omega_n} \right)^2 \right]^2 + \left[2\zeta \frac{\omega}{\omega_n} + \eta \right]^2} \right\}^{\frac{1}{2}} \tag{2.71}$$

The corresponding phase angle is:

$$\phi = \tan^{-1}\left\{ 2\zeta \frac{\omega}{\omega_n} + \eta \right\} - \tan^{-1}\left\{ \frac{2\zeta \frac{\omega}{\omega_n} + \eta}{1 - \left(\frac{\omega}{\omega_n} \right)^2} \right\} \tag{2.72}$$

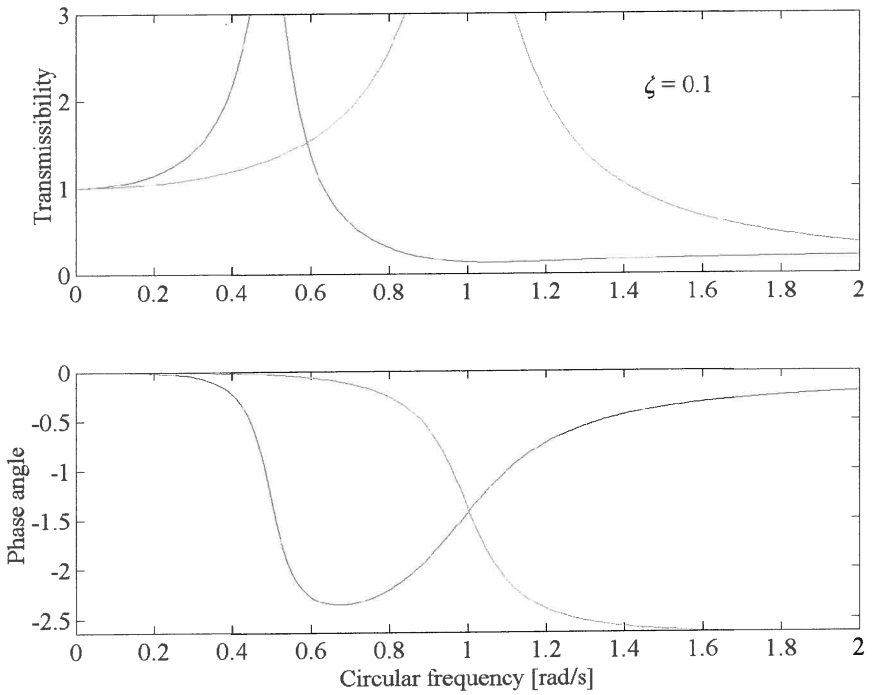

Figure 2.17 Comparison of transmissibilities with (blue) and without (green) an absorber

Figure 2.17 shows how a resonant frequency can be moved with the addition of a vibration absorber.

2.7.4 Transmissibility of system with a conical inlet/outlet geometry

As in the previous paragraphs the transmissibility is defined in terms of the applied and transmitted forces. The applied and transmitted forces defined by equations 2.24 and 2.25 can be transformed to the frequency domain using the assumed harmonic excitation and response. The result is:

$$\frac{F_o}{F_i} = \frac{k(1+i\eta)+i\omega c+\omega^2\rho\left[l-2h_c+2\frac{A_a}{A_c}\left(\frac{h_p^2}{h_p-h_c}-h_p\right)\right]\left(1-\frac{A_b}{A_a}\right)A_b}{k(1+i\eta)+i\omega c-\omega^2\left\{m+\rho A_a\left[l-2h_c+2\frac{A_a}{A_c}\left(\frac{h_p^2}{h_p-h_c}-h_p\right)\right]\left(1-\frac{A_b}{A_a}\right)^2\right\}} \tag{2.73}$$

The undamped isolation frequency is:

$$\omega_a' = \sqrt{\frac{k}{\rho\left[l-2h_c+2\frac{A_a}{A_c}\left(\frac{h_p^2}{h_p-h_c}-h_p\right)\right]\left(1-\frac{A_b}{A_a}\right)A_b}} \tag{2.74}$$

The ratio of isolation frequencies before (ω_a) and after (ω'_a) the addition of the conical inlets is:

$$\frac{\omega'_a}{\omega_a} = \sqrt{\frac{l}{l - 2h_c + 2\frac{A_a}{A_c}\left(\frac{h_p^2}{h_p - h_c} - h_p\right)}} \tag{2.75}$$

This equation shows that the conical inlet's effect can be represented by a change in length of the tuning port. The denominator in equation 2.75 is always less than the numerator. The isolation frequency of a port fitted with conical inlet/outlet will therefore always be more than for an absorber with a square inlet/outlet.

2.8 Conclusion

The LIVE absorber has rather unique properties that require careful analysis for successful design. This chapter showed that:

- An absorber will decrease the natural frequency of a system by adding mass to the system.
- Damping will have a serious detrimental effect on the achievable transmissibility. It can be controlled with diligent choice of elastomeric compound and inlet/outlet geometry.
- Changes to the inlet/outlet geometry will increase the isolation frequency.
- The ideal absorber will be designed with the natural frequency occurring as far as possible before the isolation frequency.

The next chapter will show how this analysis will be used to design an experimental absorber for evaluation.